We thank both referees for their thoughtful and thorough reviews of our paper. We appreciate you taking the time to complete these reviews and welcome your helpful comments. We have revised the manuscript to address your review comments (see below). Throughout this response to review document your (referee review) comments are provided in regular, non- italic font text, our response comments are provided in red font (as here).

Reviewer 1:

1 Summary statement

This manuscript presents simulations from different ice sheet models showing the im- pact of a potential collapse of Larsen C and George VI ice shelves on the tributary glaciers feeding them. They investigate the case of a sudden and gradual collapse, and assess the impact of different model parameters (grid resolution, sliding law, ...) on the results. They show that changes in the Larsen C ice shelf have limited impact on its tributary glaciers, as this ice shelf provides a limited amount a buttressing. A collapse of George VI ice shelf on the other hand would have a much larger impact, as it provides more buttressing to its tributary glaciers and these glaciers are resting on bedrock with retrograde slopes inland, making them prone to the marine ice sheet instability.

The results presented in this manuscript are novel and interesting, showing the very different response of glaciers in two basins, in terms of grounding line retreat and contribution to sea level change. It is great to see that this study is based on three different models, however one of them is exactly state of the art, and present results largely different to the other two, so it would be great to discuss this point and conclude on the possibility (or not) to use such simple models to investigate dynamic changes of Antarctic glaciers. Furthermore, there is not much discussion in this manuscript, just a description of the results, so it would be good to see a more substantial discussion added, including the impact of the different choices make in the model such as the sliding law used, the model resolution, and the agreement between models or between scenarios. The paper is well written and clear, except for the two tables and their captions, which are quite confusing. Below are some more detailed comments.

2 Major comments

I think it would be great to add “potential” in the title (”... to a potential collapse ...”), to highlight that this is just a possibility, or a future event. I think this is important given the recent collapse of the Larsen C iceberg, as it might confuse some people to talk about the collapse of Larsen C.

We agree with the reviewer and changed the title accordingly.

I found it confusing that the experiments are described one after the other as the text goes (new friction laws, different resolutions, ...). It would help to list all the experiments done in section 2 (maybe in 2.5 mention the additional experiments), or add a table with the list of experiments, so that the reader knows ahead of time what to expect.

We agree and have added a table listing all perturbation experiments including sensitivity simulations as well as grid resolution to the section ‘Experimental Design’ (Section 2.5).

In section 2.4, it is stated that the models should start with an initial state as close as possible from a steady-state. I disagree with this statement; the goal of the initialization is to get as close as possible to the conditions at a given time, including the thinning rate observed at this time. Removing this thinning/thickening rate can lead to an

underestimation/overestimation of the changes simulated, especially as this kind of signal would probably take decades to fade out. Also, how large is the flux correction applied to the models and how does it impact the simulations and the conclusions of this paper.

The reviewer is correct that if the ice sheet is not in steady state then there should be a thinning/thickening rate after the initialisation. As the goal of this study is to tease out the contribution from ice-shelf removal to sea-level rise projections, we want an ice-sheet geometry that does not change over time. This is why we apply the synthetic mass balance to keep the geometry as close as possible to the initial geometry. To make this clearer in the manuscript we changed the first paragraph of the 'Spin-Up' section. It reads as follows: "Following initialisation the sheet-shelf models should be close to equilibrium if the ice sheet is close to steady state, providing dh/dt = 0. However, owing to data inconsistencies and in part a violation of this steady-state assumption this condition is not fulfilled, requiring a spin-up or relaxation simulation to reach a steady state for each model. To tease out the sea-level rise contributions from ice-shelf removal and facilitate comparison across all three ice-sheet models, the employed spin-up approach aims to keep the ice sheet geometry as close as possible to the initial geometry. "

p.10 l.2: I have a different interpretation of the Pattyn et al. (2013) paper. If steady-state grounding line positions are well captured with an internal flux condition, the paper states that "the short-time transient behavior is then incorrect" (abstract of Pattyn et al. (2013)). So such models might be less dependent to grid resolution but it does not mean that they are accurate.

We agree with the reviewer that the short-term transient behaviour of these hybrid models with an internal flux boundary condition may not be correct. However, in most of our perturbation simulations quasi steady-state is reached with PSU3D, meaning that steady-state grounding line positions should agree better between PSU3D and BISICLES after 300 years. The sentence is just stating that grid dependence is much reduced in PSU3D in comparison to BISICLES. As the Pattyn et al. (2013) paper is not the best citation for this, we have removed it from the revised manuscript.

Fig.7 shows that for some basins and variables, there is a good agreement between the PSU3D and BISICLES models for the different scenarios, while in other cases, there is a bigger difference between the two models that between the different scenarios. This should be better discussed, especially to highlight the reasons of these differences as well as the different cases. Section 3 describes these results, but there should be some discussion summarizing these findings.

We have added a paragraph to the discussion section to discuss the differences in results more in depth. It reads: "We attribute the good agreement across both models for Larsen C to the fact that the area of the marine-based sectors is limited in this domain (2.1 mm contained in marine-based sectors) due to the very mountainous bedrock topography constraining potential grounding-line retreat. This is supported by all simulations across all ice-sheet models as even under a wide range of different forcings the Larsen C embayment does not contribute more than 4.2 mm by 2300. The greater potential to initiate grounding-line retreat is presented by George VI Ice Shelf where much of the ice sheet is marine based with retrograde sloping bedrock topography (Figure 1b). As this large grounding-line retreat is only initiated in the BISICLES simulation, large differences in sea-level rise projections occur. The most likely scenario for this differing behaviour is due to the difference in the inferred basal traction coefficient fields that affects each model's response to ice-shelf removal. PSU3D predicts much stickier bedrock conditions in the George VI embayment than BISICLES (Figure 2). These sticky bedrock conditions result in

little acceleration of the major outlet glaciers following ice-shelf breakup. This in turn means that the calving law applied to only floating ice cells cannot drive the initial retreat into the marine based sectors as the outlet glaciers do not thin sufficiently to form a floating ice tongue. In contrast in the RCP8.5 BISICLES simulation for George VI, speed-up in response to ice-shelf breakup leads to enhanced dynamic thinning of the main outlet glaciers. This thinning in conjunction with the calving law drives the calving front into the marine-based sectors where further retreat is initiated by a combination of the marine ice-sheet instability and the meltwater driven calving law, resulting in the simulated much higher sea-level rise projections."

Overall, there is no real discussion, just a description of the results. A proper discussion should include the current limitations of the models and future possible improvements, the impact of the different models compared to other parameters, such as the sliding law employed, the scenario chosen, or the bedrock used, with references to previous studies.

We have added a paragraph to section 3.3. that discusses and highlights the model limitation, key parameter uncertainties and improvements for future studies. It reads: "In addition, our experiments show that for simulations of grounding-line motion in response to ice-shelf breakup sheet-shelf models are necessary. The simple model BAS-APISM fails to reproduce the results of the sheet-shelf models due to the simplified physics. Even across sheet-shelf models differences in model physics, model initialisation, calving law implementation and other numerics (e.g. meshing) can lead to substantially different projections under the same forcing (Figure A5). Sea-level rise projections are most sensitive to the choice of sliding law and bedrock geometry. The peninsula is not the only region where these parameters highly affect decadal to centennial sea-level rise projections as similar conclusions were drawn from modelling of outlet glaciers in the Amundsen Sea embayment (Nias et al., 2018). The wide range of sea-level rise responses to different forcing parameters underlines the need for perturbed ensembles to explore key parameter uncertainties (e.g. basal sliding law) for sea-level rise projections in greater detail for the peninsula region. Owing to the increase in computer power these type of ensemble projections have become feasible at the regional (e.g. Nias et al., 2016) and continental scale (e.g. DeConto and Pollard, 2016).

3 Specific comments

p.1 l.1: "past several": be more precise

changed to "past five decades"

p.1 l.13: "northerly limit": it would be great to explain this limit in a few words

we added "… determined by the -9°C mean annual isotherm…"

Fig.1: "meters above sea level" is a bit confusing as all elevations are negative, maybe simply saying "in meters" would be enough. Also mention that the colorbar is truncated at 0, and maybe add the highest elevation in this area. The black polygons are not clear and can be confused with the grounding line position, consider using a different color or thick lines.

We have changed the text and figure accordingly. Black polygon lines have been made thicker and we simply state now "…elevations below sea level in meters".

p.2 l.7: mention that happens on downward sloping bedrock elevation inland (not just on all marine based sectors)

We added "…and retrograde sloping bedrock topography…"

p.2 l.9: remove “state-of-the-art” as I am not sure that the BAS-APISM model can be considered to be a state-of-the-art model (“simulates ice flow by solving the simplest permissible force basal approximation” p.3 l.7)
Removed
p.2 l.10: same as the title: add that you are talking about a potential collapse
Done
p.3 l.10: “SIA is not valid at the grounding line”, the problem here is rather that SIA is not valid on floating ice shelves and fast flowing ice streams.
Changed to: “As the SIA is not valid for floating ice shelves, …”
p.3 l.16: “in assumed” → “is assumed”
Changed
p.3 l.34: Add sentences in the three model descriptions about the grid resolution (and grid resolution at the grounding line) employed in these three models.
We have added this information to the table where all simulations are listed.
p.4 Eq.1: What basal conditions (friction) is used for the BAS-APISM model?
We added a sentence specifying that due to the linearisation there is no need to specify whether or not basal sliding is occurring. It reads: “Due to the linearisation of the evolution equations in BAS-APISM, there is no need to specify whether or not basal sliding is occurring. All rates are determined by the ice flux which is directly derived from the data.”
p.5 l.20: What is R exactly and how does it relate to the temperature in a few words?
We added: “This formula scales surface melt exponentially with mean DJF near surface temperatures …”
p.5 l.24-25: How is this done (in a sentence or two)? Some technical explanations are missing.
We have added a sentence saying: “This is accomplished through the computation of balance fluxes.”
p.6 l.18: ALBMAP is quite old, why not use the new BEDMAP2 or Huss and Farinotti, (2014) data for all the models?
The difference in ice volume and bedrock topography between ALBMAP and BEDMAP2 for the Antarctic Peninsula is rather small (<15%) and the Huss and Farinotti (2014) dataset is only available for the Larsen C domain as it does not cover the southern part of the peninsula. To gauge the importance of differences in bedrock topography, we carried out the sensitivity simulation with BISICLES for the Larsen C domain. As the difference between BEDMAP2 and the Huss and Farinotti (2014) dataset is large (~100% in ice volume below sea level), large differences propagate into the magnitude of the sea-level rise projections.
p.6 l.23: As mentioned above, do you really want the simulations to start from a steady-state? Or from the current thinning/thickening rate? Why not correct this by adding the rate of thickness change instead of assuming that it is 0? And by the way, I don’t agree that “After initialization, the sheet-shelf models should be in equilibrium”. The models should represent the actual ice sheet state at the time captured by the initialization, so if the ice sheets where thinning, the initialization should capture and reproduce this initial thinning.
p.6 l.28: Adding this flux correction is fine, but you should show how large it is, and how large it is compared to the actual surface mass balance. Also, how different are the results if you don’t include it? What are the impacts on the simulations?
See reply above. In brief, in order to really tease out the contributions that come from ice-shelf removal alone, we desire all other signals to be as close as possible to zero. This is

why we apply the synthetic mass balance to keep the ice-sheet as close as possible to its initial geometry. Of course the results of our simulations would be different without the additional synthetic surface mass balance forcing, but comparing our projections with and without this flux term is not the goal of this study.

p.7 Fig.2: Why not show the BAS-APISM model here? I have a hard time understanding what the basal boundary condition of this model is. Also should be "Black lines denote ..."

Due to the linearization of the evolution equation there is no need to specify whether or not basal sliding is occurring and balance fluxes are used to initialise the model.

p.8 l.3: What resolutions are used? The list of experiments with their characteristics should be better detailed in the text.

We have added a table with all simulations and their respective resolution to section 2.5.

p.9 l.12: Over what period does this change happens?

We added: "… averaged over 300 years"

p.9 l.14-19: The initial conditions (ice velocity, thickness, elevation, rigidity, ...) also have an impact on the evolution of the glacier, as well as the numerical parameters (grid resolution, ...).

We added: "This discrepancy between the sheet-shelf models may be attributed to a combination of differences in initialisation and that PSU3D is not as close to steady-state as BISICLES following initialisation and spin-up."

p.9 l.14-19: What about the BAS-APISM model?

As there is no time-dependent grounding-line migration after the initial perturbation, we focus on the sheet shelf models, but state at the end of the paragraph that BAS-APISM projects similar magnitudes of sea-level rise, but the spatial thinning pattern is very different to the sheet-shelf models.

p.10 Fig.4: Should be: "Upper panels (a,b) show ...", same for "Lower panels ..."

Changed

p.10 l.2: As mentioned above, the Pattyn et al. (2013) paper says that "the short-time transient behavior is then incorrect" for grounding line evolution captured with internal flux conditions.

See reply above. We have removed the Pattyn et al. (2013) citation.

p.11 Fig.5: Should be: "Black lines denote ...". Same for caption in Fig.6.

Changed

p.15 l.3: "A consequence of this is ..." → "A consequence is ..."

Changed

p.15 l.23: "most of grounding-line retreat" → "most of the grounding-line retreat"

Changed

Tables 1 and 2: the tables and their captions are quite confusing. Especially as all numbers reflect different time periods, and some variables are not standard (e.g., dGt/dt for mass change rate). Also why not use the same order as Fig.6 (BAS-APISM left, ...).

As suggested by the second reviewer, we have moved the tables to the Supplementary material as they disrupted the flow of the paper. We also changed the dGt/dt to the correct dM/dt and the respective units (if not unitless) are provided in the table caption. We also changed the order of the columns to follow the order of Figures 6 and 8 for Experiment 1 and Experiment 2, respectively. Moreover, we now present a separate table for George VI and Larsen C basins and added the Coulomb sliding BISICLES simulation for Experiment 1 to Table S1.

Table 2: Fig.A7 shows larger grounding line retreat for many glaciers (GeoIII, GeoIV, ...) with the Coulomb friction law, which does not seemed to be reflected in this table. But as I just

mentioned above, I am quite confused by this table. I would also expect this increased grounding line retreat to transfer in more mass change for the Coulomb case. It would be simpler to have both BISICLES cases next to each other.
Due to the confusing layout, the reviewer confused Experiments 1 and 2 here. They do show larger grounding-line retreat but only in comparison to other simulations from Experiment 1, but not in comparison to Experiment 2. We added the Coulomb sliding BISICLES simulation for Experiment 1 to Table S1 to make this clearer.
p.18: As mentioned previously, there is not much discussion, just a description of the results.
See reply above.
p.19 l.6: "vulnerability of ice-shelf ..." → "vulnerability to ice-shelf .."
Changed
Fig.A1: Y-axis label should be "Temp. bias" not "Temp.". Caption should detail bias which two quantities.
Fig.A2: Same as Fig.A1
Changed and added "…in relation to ERA-Interim."
Fig. A6: Caption should be "Upper panels (a,b) show ...". Same for "Lower panels ..."
Changed
Fig. A7: Simulations with Coulomb friction show a larger retreat, which is not captured in Table 2.
It is captured. See reply above.

Reviewer 2:
General comments
April 12, 2018
This paper from Clemens Schannwell and his colleagues investigates, in a timely manner, the response of the Antarctic Penisula glaciers to a collapse of the Larsen C and Georges VI ice shelves. They use three types of numerical models of different complexity applied to two main experiments, supplemented by secondary experiments. Experiment 1 starts without ice shelves, as if an ice shelf collapse had already occurred, Experiment 2 starts with the current geometry and use a calving law and potentially leads to ice shelf collapse, depending on future scenarios, which are either RCP4.5 or RCP8.5. The secondary experiments helps to quantify uncertainties, and are built upon Experiment 2 to which was added mild or strong sub-shelf melting, and a last experiment use another dataset for ice geometry (the one of Huss and Farinotti 2014) instead of the classical Bedmap2 dataset used elsewhere in the study. All those experiments are simulated from today to 2300.
I find this study very interesting and I think this can be published with minor revisions. The fact of applying different types of ice sheet models, having not only different physics for time evolutive simulations but also different approaches for building the initial spin-up (inversion + relaxation), to the same case of study is not easy but it makes the results more robust. The paper is globally well written apart from some details on which you will have specific comments below. The description of the methods is quite clear, even though it lacks the definition of Glen's flow law from which the authors could introduce the enhancing factor, which should be defined clearly.
I first have a couple of minor concerns:
- The Spin-up for BISICLES at a 1000m resolution looks odd from Figure3, the results doesn't seem to converge with the resolution (dvdt at 0 very rapidly for 4000, 2000 and 500m resolutions, but quite different for 1000m). Did you, by any chance, accidently shift, say, the

colors for 4000m and 1000m??? If not, could you make a few comments on that in the paper.

We did not expect convergence in the spin-up simulations by increasing the mesh resolution. These simulations all use a synthetic surface mass balance that is derived from their respective model grids after one timestep. In some of the simulations, the model drift and the remaining thinning/thickening signal following initialisation may not be as well captured after one timestep as in others (e.g. 2000 m vs. 1000 m BISICLES). In addition, the initialisations were performed also on different grids (1 km for BISICLES and 5 km for PSU3D). All in all, these factors most likely lead to the slightly different dV/dt patterns that are shown in Figure 3. Considering that steady-states with real world geometries are difficult to achieve, we are satisfied with how close they are to steady state after relaxation. PUS3D could not be run at higher resolution as it became unstable at resolutions of < 1000 m. Therefore, we chose 1000 m.

- I was not always sure about the type of SMB that you applied, for the spin-up but also for the experiments. You introduce the Albmap SMB but in the inversion process, not in the spin-up neither in the description of transients. Make it more clear in the text.

We have added a sentence to section 2.4 that clarifies that we use the synthetic mass balance for all experiments. It reads: "This synthetic mass balance is applied in all spin-up and perturbation simulations."

- Could you change the time origin in the evolutive plots to be 2000 instead of 0?

Changed accordingly

- Could you mention that sub-shelf melting is always 0 (if I understood correctly), apart from your two additional experiments.

We added a sentence to section 2.5. to clarify this. It reads: "Moreover, ocean melting is set to zero in the perturbation experiments unless stated otherwise."

- I would be glad if you could indicate the position of the calving front in your maps of Experiment2 results, for 2100 and 2300 for instance, or maybe, if it's more easy, indicate the year of collapse in Figure7. This would strongly help the understanding of ice dynamics differences between Exp1 and Exp2.

We think that adding the calving front to Figure 8 at these two timesteps would clutter up the Figure too much. Moreover, the calving front in 2300 is very close to the grounding-line that is drawn in Figure 8 anyway. Rather than visualise the calving front with lines in Figure 8, we find the ice-shelf area loss plots (Figure 7e, f) more informative as the evolution of ice-shelf retreat can be tracked better over time. In addition to these plots, we added a sentence that states that once the ice shelf has collapsed, grounding-line and calving front are almost in identical locations.

- I would be in favor of adding a table to summarise all the experiments, including the main exp1 and Exp2 but also the three others.

We have added a table listing all experiment and the resolutions at which they were run to section 2.5.

- I would also be in favor of adding those results to Table2, and put the two tables in the supplementary, to help the reading and understanding of what has been done.

Yes, we moved the tables to the Supplementary as they disrupted the flow of the paper. We also changed the dGt/dt to the correct dM/dt and the respective units (if not unitless) are provided in the table caption. We also changed the order of the columns to follow the order of Figures 6 and 8 for Experiment 1 and Experiment 2 respectively. Moreover, we now present a separate table for George VI and Larsen C basins and added the Coulomb sliding BISICLES simulation for Experiment 1 to Table S1.

- Some assertions are not always correct in the reading of the results (see below)
The rest of my review is a series of specific comments and recommmendations, which would like to be followed as well.

Specific comments

Page1

l17: Could you mention those other mechanisms?

We added "… such as ice-shelf thinning, fracturing, and weakening of shear margins …"

l18: Could you add a word like "slightly" just before increased? This is at least what I understand from the Jansen et al., 2015 study

Done

Page2

Figure 1:

- The Y label should be "elevation [m a.s.l]"
- In the caption, "localities mentioned in the text"
- In the caption, remove "below sea level"
- In the caption, replace "Black polygons..." by something like "The grounded part of the ice sheet only is represented"

We have changed to "localities in the text" and followed the suggestions from reviewer 1. Black polygon lines have been made thicker and we simply state now "…elevations below sea level in meters".

l8: "a tendency...": Here the way this instability works doesn't appear clearly. Nowhere there is written that you have deepening of the bedrock towards the interior, which is a necessary condition (at the necessary condition that bedrock is below sea level) to a MISI. Be more precise please.

We added "…and retrograde sloping bedrock topography…"

Page3

l10: Why is the SIA not valid at the grounding line? could you mention the reason or/and add a citation here ?

We have added a citation to (Hutter, 1983)

l21: The way this is said, it is not clear whether the condition is imposed at the grounding line, to me at least... Could you rephrase.

We have added "… is employed at the grounding line."

Page4

l11: Is there a reason to take 0.5 specifically? Tsai et al., advises f<0.6, Brondex et al., takes 0.5. Could you make a few comments on that.

Most ice-sheet modelling studies have used a value of f=0.5 (see Asay-Davis et al. 2016, Brondex et al. 2017, Nias et al. 2018). To keep in line with this, we chose the same value for our simulations.

Page5:

l9: So the criterion in Bisicles is Height surface crevasse + Height basal crevasse = ice surface? this is not clear to me

We have rewritten to read: "…reaches the distance from ice surface to the waterline."

l12: Do you need a capital H in historical?

Changed to lower case.

l29: You should have defined this enhancement factor before reaching this part. It is worth to detail the Glen's flow law equation somewhere above, from which you can easily define the enhancement factor.

Added to the section 2.1.

Page6
l7: I am glad you showed Figure A3 (Hum, this figure reminds me Belgium...)
We added a sentence to acknowledge this. It reads: "The layout was inspired by Berger et al. (2016)."
l11: m=1 ? Something is wrong here, or is this a typo?
We added "… for the inversion simulation." We then recompute the basal drag coefficient field from the inversion (linear sliding) for the other sliding laws used in the perturbation experiments.
l18: You used SMB for the spin-up only (and alos the transient for, could you be more accurate here
This was ambiguous. We removed surface mass balance here and added a sentence to section 2.4 that clarifies that we use the synthetic mass balance for all experiments. It reads: "This synthetic mass balance is applied in all spin-up and perturbation simulations."
Page7
Figure 2: Is that the PSU3D grid that we can distinguish in Figure2? Why is that so?
We do not know what the reviewer means by this. No grids are shown in Figure 2. Only the outline of our model domain (black polygon) is visible.
l4: " In the first simulation (hereafter Experiment 1)" -> in Experiment 1?
Changed.
l5: This is not clear what you took for SMB in Experiment 1?
We added a sentence to section 2.4 that clarifies that we use the synthetic mass balance for all experiments. It reads: "This synthetic mass balance is applied in all spin-up and perturbation simulations."
Page8
Figure3:
- Isn't that curious that the 1000m resolution results for BISICLES are outlying compared to the others? I would have expected the results to converge when getting closer to 500m resolution, but it is not the case here. Could you discuss that?
- The solution of PSU3D is not really converging. The model can't be applied at a lower resolution? Could you add few comments on that if you find it relevant.
We did not expect convergence in the spin-up simulations by increasing the mesh resolution. These simulations all use a synthetic surface mass balance that is derived from their respective model grids after one timestep. In some of the simulations, the model drift and the remaining thinning/thickening signal following initialisation may not be as well captured after one timestep as in others (e.g. 2000 m vs. 1000 m BISICLES). In addition, the initialisations were performed also on different grids (1 km for BISICLES and 5 km for PSU3D). All in all, these factors most likely lead to the slightly different dV/dt patterns that are shown in Figure 3. Considering that steady-states with real world geometries are difficult to achieve, we are satisfied with how close they are to steady state after relaxation. PUS3D could not be run at higher resolution as it became unstable at resolutions of < 1000 m. Therefore, we chose 1000 m.
l1: "best available": I don't think this is relevant to say so, no offense...
Deleted.
Page9
l5: Results and discussion
l12: Sea-level rise by 2100?
For clarity we added: "…by 2300."

l17: The differences in terms of sea level response may be due to those large differences that you have between friction coefficients fields?
We have rewritten this sentence. It reads: "This discrepancy between the sheet-shelf models may be attributed to a combination of differences in initialisation, inferred basal traction fields, and that PSU3D is not as close to steady-state as BISICLES following initialisation and spin-up."
l18: Could you maybe detail the relevant specific differences?
We have extended this paragraph to accommodate this. It reads: "Such a response has been previously attributed to differences in the underlying model physics (L1L2, A-HySSA). Using synthetic geometries, A-HySSA models have shown to be more sensitive to grounding-line advance as well as retreat. These differences are most likely caused by the neglecting of vertical shearing terms in the pure membrane ice-sheet models (Pattyn et al., 2013)."
Page10
Figure4: Could you start your time scale at 2000?
Changed.
l1: where do we see the dependence to grid resolution in Figure A4? This is rather observed in Figure A6.
Changed.
And according to Figure A6, there is also a sea level contribution dependency to grid resolution in PSU3D. Moreover, this is true that this dependency is small for Georges VI (not absent though) and comparable to BISICLES for Larsen C. Could you rephrase here.
We rephrased to: "… much reduced …"
l4: you definitely refer to Figure A6
Yes, we changed it accordingly.
Page11
Figure5: It seems that the 2000 grounding line is slightly different between PSU3D and BISICLES. The differences are difficult to quantify, so could you maybe write down somewhere the maximum difference between initial grounding lines for the two models?
We state in section 3.2 that the effect of the more advanced grounding-line position in PSU3D for the Larsen C domain accounts for a sea-level equivalent of 0.28 mm. We find this number more informative than a maximum difference in grounding-line position and therefore would like to keep it.
l10: A necessary condition to have a MISI is a retrograde bed slope, insofar as you have a marine based basin as well. You thus need to replace "mostly marine-based outlet" by "retrograde bed slope something..."
Changed
l13: Could you discuss this a bit more. There is this paper from Gudmundsson et al., in 2012 and Gudmundsson in 2013 about the buttressing provided by an ice shelf to its upstream glacier as a function of the grounding line gate width...
This is a good point. We have extended the paragraph to discuss this now. It reads: "These findings suggest that stabilising forces such as basal and lateral drag may provide enough resistance for the ice sheet in western Palmer Land to remain in a stable configuration following the initial response to ice-shelf collapse. This is supported by earlier modelling studies with idealised geometries, showing that the magnitude of grounding-line retreat is a function of the retrograde sloping channel width (Gudmundsson et al., 2012, Gudmundsson et al., 2013). The smaller the channel width, the less retreat was simulated (Gudmundsson et al., 2012). Considering the small size of the drainage basins in the

peninsula region with channel widths <30 km, the remaining lateral buttressing from shear margins likely impedes any runaway grounding-line retreat."

Page12

l3: "dependent"

Fixed.

l7: Remove "fixed calving front simulation, immediate shelf-collapse scenario" and keep "Experiment 1"

Changed.

l10: Remove "just"

Removed.

l10: "the larger" -> "the largest"

We think "the larger" is correct.

Page13

Figure7: Time between 2000 and 2300

Changed

l1: "projections ... agree well": this is not really what I see in Figure7a, where the two models may agree for the first 50 to 70 years, but not really for the rest of the simulations. Could you rephrase?

We added "…reasonably well …"

l4: "BISICLES projects no slr for RCP4.5": more correct would be to say "small" or "limited" instead of "no", especially for Larsen C

Changed to "little"

Page14

l1: "Both sheet-shelf models project similar sea-level rise by the mid 22nd century in Experiment 2": Again, I don't agree with this sentence, after 250 years Larsen C ice loss is 0.25 and 0.6 for BISICLES4.5 and PSU3D4.5, and this is not the only example where I find differences where you write the opposite (see above). You should rewrite here.

Sorry this statement was meant for the George VI embayment. We have added a qualifier at the end of the sentence: "… for the George VI domain…" We also meant 2150 with "the mid 22nd century". To avoid any confusion, we changed this phrase to 2150.

l2: What do you mean by "forced back"? Does it simply mean that the grounding line retreat? Could you rephrase?

Yes. We changed this to read: "…grounding lines retreat further back into …"

l3: "because a fixed calving front": Here I dont 'understand, the fact of having a fixed calving front does not prevent the retreat of the grounding line. You need to rephrase.

Yes, we have rephrased it. After ice-shelf collapse grounding line and calving front are in almost identical locations. To highlight this, we added: "After ice-shelf collapse, grounding line and calving front for all drainage basins are almost in identical locations."

l1 to l14: For this paragraph, this is not cristal clear to me if you talk about Georges VI or Larsen C ice shelf. Can you make the text more clear please.

Yes, it was not very clear. We rewrote sections of the paragraph and also added a paragraph to discuss the difference in projections across the models.

l25: Don't understand this sentence. you say that your model show a strong dependence to what? Calving criteria or sub-shelf melting

We rephrased this to read: "…in other words, it is ice-shelf break-up in combination with the calving criteria that dominates our results."

Page15

l3: Ok, this is another experiment. I recommend to add a table to summarize all the experiments

Done. See above.

l8: five more drainage basins, means not the LarI to LarV and GeoI to GeoV? could you indicate in a figure which are the supplementary basins that you accounted for ? Maybe put it into Figure8?

Apologies this was ambiguous. We indeed mean the basins LarI to LarV and GeoI to GeoV. This sentence was changed to improve clarity. It reads: "To further assess the impact of ice-shelf break-up, five drainage basins from the Larsen C embayment (LarI-LarV, Figure 8) and George VI embayment (GeoI-GeoV, Figure 8) were selected for additional analysis."

Page17

Table1: What did you put in parenthesis from the dGL and dGt/dt columns? Does it correspond to the year you had the maximum speed up? You need to write it down then.

Table1 and Table2: Would you like to move those 2 tables in the Supplementary? I have the feeling that it affects the reading of the paper...

Yes, we moved the tables to the Supplementary as they disrupted the flow of the paper. We also changed the dGt/dt to the correct dM/dt and the respective units (if not unitless) are provided in table caption. We also changed the order of the columns to follow the order of Figures 6 and 8 for Experiment 1 and Experiment 2 respectively. Moreover, we now present a separate table for George VI and Larsen C basins and added the Coulomb sliding BISICLES simulation for Experiment 1 to Table S1.

Page19

l4: You definitely need to show your results with the Fuss and Farinotti geometry

The Huss and Farinotti results have been added to Figure 4

Suplementary

Figure A3: Could you explain why you chose $\lambda_C = 10^{-1}$? It doesn't seem that obvious looking at A3c. Stupid question maybe, why is there a jump between 10^{-1} and 10^{1} (I mean no 10^{0} appearing)?

Apologies. The exponent 0 was missing. This is now fixed. We chose 10^{-1} because we wanted to make sure that we are close to the kink of the L but still on the lower branch. 10^{0} was too close to the kink in our opinion.

FigureA6: Time origin should be 2000

Changed accordingly.

We amend the following sentence to the manuscript acknowledgements, to read: 'We thank the editor Olivier Gagliardini, Lionel Favier, and an anonymous reviewer for comments which improved the manuscript.'.

Clemens Schannwell

Dynamic response of Antarctic Peninsula Ice Sheet to potential collapse of Larsen C and George VI ice shelves

Clemens Schannwell[1,2], Stephen Cornford[3], David Pollard[4], and Nicholas Edward Barrand[1]

[1]School of Geography, Earth and Environmental Sciences, University of Birmingham, Birmingham, UK
[2]British Antarctic Survey, Natural Environment Research Council, Cambridge, UK
[3]Centre for Polar Observation and Modelling, School of Geographical Sciences, University of Bristol, Bristol, UK
[4]Earth and Environmental Systems Institute, Pennsylvania State University, University Park, PA, USA

Correspondence to: Clemens Schannwell (Clemens.Schannwell@uni-tuebingen.de)

Abstract. Ice shelf break-up and disintegration events over the past ~~several~~ five decades have led to speed-up, thinning, and retreat of upstream tributary glaciers and increases to rates of global sea-level rise. The southward progression of these episodes indicates a climatic cause, and in turn suggests that the larger Larsen C and George VI ice shelves may undergo similar collapse in future. However, the extent to which removal of Larsen C and George VI ice shelves will affect upstream tributary glaciers and add to global sea levels is unknown. Here we apply numerical ice-sheet models of varying complexity to show that the centennial sea-level commitment of Larsen C embayment glaciers following immediate shelf collapse is low (<2.5 mm to 2100, <~~4.3~~4.2 mm to 2300). Despite its large size, Larsen C does not provide strong buttressing forces to upstream basins and its collapse does not result in large additional discharge from its tributary glaciers in any of our model scenarios. In contrast, the response of inland glaciers to collapse of George VI Ice Shelf may add up to 8 mm to global sea levels by 2100 and 22 mm by 2300 due in part to the mechanism of marine ice sheet instability. Our results demonstrate the varying and relative importance to sea level of the large Antarctic Peninsula ice shelves considered to present a risk of collapse.

1 Introduction

The observational history of ice-shelf collapse in the Antarctic Peninsula has led to a proposed northerly limit of ice-shelf viability determined by ~~climate~~ the -9°C mean annual isotherm (Mercer, 1978; Morris and Vaughan, 2003). Recent, rapid warming has led to the southward migration of this limit (Vaughan et al., 2003), now threatening the stability of the large Larsen C and George VI ice shelves. The northernmost remaining ice shelf (Figure 1a), Larsen C, is considered to present the greatest risk of collapse (Jansen et al., 2015). While other mechanisms such as ice-shelf thinning, fracturing, and weakening of shear margins may contribute to Larsen C ice-shelf ~~stability~~ instability (Kulessa et al., 2014; Holland et al., 2015; Borstad et al., 2016), the risk of shelf collapse has increased slightly since summer 2017 when a large iceberg calved off Larsen C. This calving event leaves Larsen C in conditions similar to those present immediately prior to the collapse of Larsen B Ice Shelf in 2002 and may promote instability (Jansen et al., 2015).

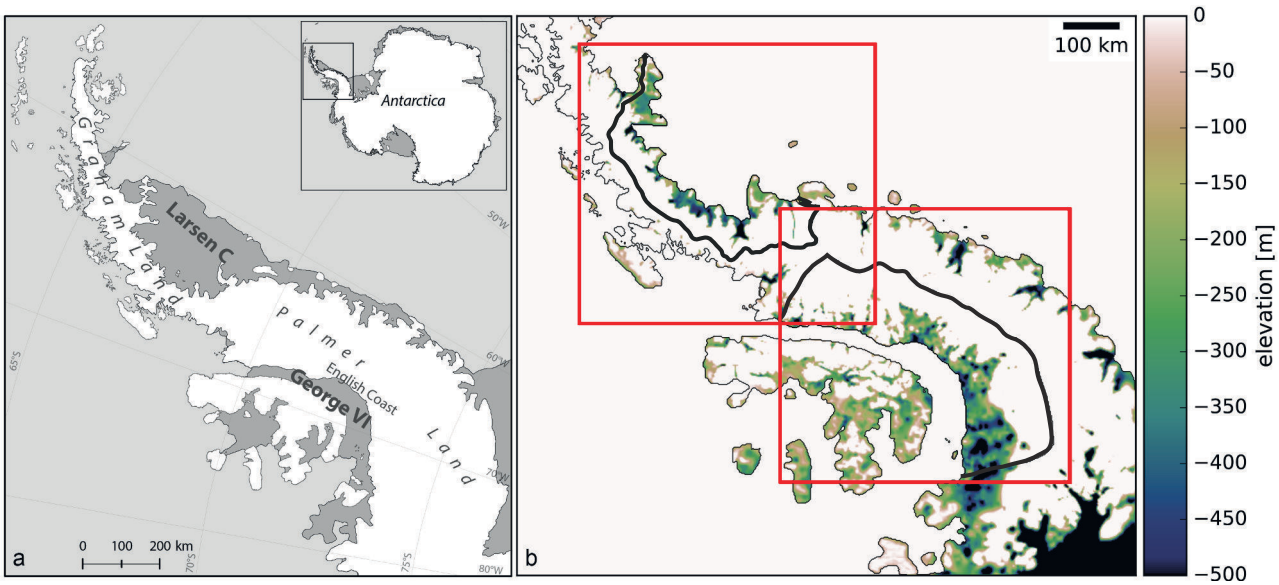

Figure 1. (a) Location map of the Antarctic Peninsula including locations of Larsen C and George VI ice shelves and localities mentioned in the text. (b) Bedrock elevations below sea level (in meters ~~above sea level (m a.s.l))~~ for the Antarctic Peninsula from BEDMAP2 (Fretwell et al., 2013). The colourbar is truncated at 0 m. Red inset rectangles delineate location of zoom-in views in Figure 8. Black polygons denote ice-sheet model domains.

Despite the increased research focus on Larsen C Ice Shelf, most of the current mass loss and contribution to sea-level rise from the Antarctic Peninsula originates from large drainage basins feeding George VI ice shelf, along the English Coast, western Palmer Land, in the south-west of the peninsula (McMillan et al., 2014; Martín-Español et al., 2016). Here, outlet glaciers have thinned rapidly in the last two decades, contributing ∼0.1 mm a^{-1} to global sea-level rise (Wouters et al., 2015; Hogg et al., 2017). Many of these glaciers are grounded below sea-level with deeply-incised bedrock troughs and retrograde sloping bedrock topography (Figure 1b). These marine-based sectors, which contain a sea-level equivalent of 46.2 mm (25% of the total ice volume in the APIS, Figure 1b), are therefore potentially vulnerable to the marine ice sheet instability mechanism, a tendency of grounding-line retreat to accelerate in the absence of compensating forces (Schoof, 2007; Gudmundsson et al., 2012).

Here we use three ~~state-of-the-art~~ ice-sheet models of varying complexity to compute the upstream glacier response and sea-level rise commitment following potential collapse of Larsen C and George VI ice shelves. Owing to differences in model setup and physics, this study does not provide a full model intercomparison, but rather presents a multi-model spread sea-level envelope assessment using a range of ice-flow approximations: (i) the linearised shallow-ice approximation (SIA) model BAS-APISM (Barrand et al., 2013); (ii) the hybrid sheet-shelf model PSU3D (Pollard and DeConto, 2012a), and; (iii) the vertically-integrated sheet-shelf model BISICLES (Cornford et al., 2013). This multi-model approach provides a starting point for regional ice-sheet model forecasts and sea-level impact studies and allows examination of process differences in glacier responses across the drainage basins of Larsen C and George VI ice shelves.

2 Methods

The ice-sheet models BAS-APISM (Barrand et al., 2013), BISICLES (Cornford et al., 2013), and PSU3D (Pollard and DeConto, 2012a) have been described in detail elsewhere. A summary of model description, parameterisation and experimental design relevant to this study are presented here, including important changes to model setups from previously published configurations.

2.1 Ice-sheet model description

BAS-APISM (Barrand et al., 2013) simulates ice flow by solving the simplest permissible force balance approximation - the linearised shallow-ice approximation (SIA). Owing to the linearisation, the model is less sensitive to ice thickness errors than traditional SIA-based models. The linear nature of the model equations permits simple summation of sea-level rise contributions from individual drainage basins to provide an ice-sheet wide estimate. As the SIA is not valid ~~at the grounding line~~for floating ice shelves (Hutter, 1983), only the grounded ice sheet is simulated and grounding-line retreat is parameterised through a statistical model. This model scales the expected retreat of the grounding line in response to ice-shelf collapse to the amount of buttressing at the ice front of each drainage basin (Schannwell et al., 2016). Ice-shelf buttressing was computed from output of an ice-sheet model inversion (Arthern et al., 2015). As BAS-APISM cannot simulate grounding-line advance, ice-shelf flow, or ice-shelf buttressing, this model is only employed in Experiment 1 (immediate ice-shelf collapse) where ice-shelf flow is not explicitly simulated (See Section 2.5) and immediate ice-shelf collapse ~~in~~ is assumed.

PSU3D (Pollard and DeConto, 2012a) simulates ice flow by using a hybrid combination of the scaled SIA and shallow-shelf approximation (SSA) equations. The SSA is valid for ice shelves and ice streams characterised by low basal drag. This type of ice-sheet model (A-HySSA = asymptotic hybrid SIA-SSA model (Pattyn et al., 2013)) provides the required physics to simulate the ice sheet-ice shelf system, including explicit tracking of the position of the grounding line. To make the model less sensitive to grid resolution~~at the grounding line~~, an additional internal flux boundary condition is employed at the grounding line. The model set-up used here is similar to Pollard et al. (2015), but cliff failure and bedrock deformation are not included. PSU3D solves the time varying 3-D temperature equation, but surface air temperature forcing is held constant at year 2000 (Le Brocq et al., 2010) throughout the simulations.

BISICLES (Cornford et al., 2013) simulates ice flow by solving a vertically integrated stress balance (L1L2 = one-layer longitudinal stress model (Hindmarsh, 2004)) to determine the horizontal velocity. The ice rheology is given by Glen's flow law

$$\boldsymbol{S} = 2\phi\eta\dot{\boldsymbol{\epsilon}}. \tag{1}$$

Here $\boldsymbol{S}$ is the deviatoric stress tensor, η is the effective viscosity , $\dot{\boldsymbol{\epsilon}}$ is the strain-rate tensor and ϕ is the stiffening factor that accounts for ice damage, anisotropy, and temperature uncertainties (Cornford et al., 2015). This type of stress balance is similar to the SSA, but includes vertical shearing in the effective viscosity calculation, resulting in softer ice at the grounding line in comparison to traditional SSA models and resembles more the behaviour of full-Stokes models (Pattyn and Durand, 2013). The

equations are solved on an adaptive 2-D grid, allowing for higher resolution in areas of interest such as grounding lines or shear margins, and coarser resolution away from these regions to save computation time. A subgrid interpolation scheme for basal drag near the grounding line was employed to improve the accuracy of the grounding-line position at each time step (Cornford et al., 2016). In all BISICLES simulations ice temperature data are provided by a three-dimensional thermo-mechanical model (Pattyn, 2010) and is held fixed in time.

Basal traction in PSU3D and BISICLES is determined by a viscous law

$$\tau^b = \begin{cases} -C|\boldsymbol{u}|^{m-1}\boldsymbol{u} & \text{if } \frac{\rho_i}{\rho_w}h > -b, \\ 0 & \text{otherwise,} \end{cases} \tag{2}$$

where m=0.5 (quadratic law), τ^b is the basal traction, $\boldsymbol{u}$ is the horizontal velocity, ρ_i and ρ_w are ice and ocean densities, b is the bedrock elevation, h is ice thickness, and C is the basal friction parameter inferred by solving an inverse problem (See Section 2.3). Due to the linearisation of the evolution equations in BAS-APISM, there is no need to specify whether or not basal sliding is occurring. All rates are determined by the ice flux which is directly derived from the data (Barrand et al., 2013)

Basal sliding sensitivity simulations with BISICLES were also performed with m=1/3 (cubic law) and m=1 (linear law). In addition, a simulation was performed using a Coulomb-limited law (Tsai et al., 2015). This law combines the power law (Equation 2) with the Coulomb friction law by ensuring that basal traction cannot exceed the Coulomb friction that is proportional to the effective pressure N_e:

$$|\tau_b| = \min\left(aN_e, C|\boldsymbol{u}|^m\right), \tag{3}$$

where the first term in the parentheses is the Coulomb friction law with a=0.5, m=0.5 and the effective pressure N_e is

$$N_e = \rho_i g(h - h_f), \tag{4}$$

where g is the acceleration of gravity and h_f is the flotation thickness. Equation 4 is only valid under the assumption of full connection between the basal hydrology and the ocean. Since the Coulomb law implies that basal drag approaches zero towards the grounding line, this type of basal sliding law ensures a smooth transition from grounded to floating ice, unlike the traditional power law (Equation 2) which implies that basal drag is highest near the grounding line (Tsai et al., 2015).

2.2 Calving

In simulations where the calving front is not fixed e.g. where ice-shelf flow and retreat is explicitly simulated, calving depends on the depths of surface (d_s) and basal crevasses (d_b), relative to total ice thickness. Crevasse depths are computed by (Benn et al., 2007; Nick et al., 2010)

$$d_s = \frac{2}{\rho_i g}\left(\frac{\dot{\epsilon}}{\bar{A}}\right)^{\frac{1}{n}} + \frac{\rho_w}{\rho_i}d_w, \tag{5}$$

$$d_b = \left(\frac{\rho_i}{\rho_0 - \rho_i}\right)\frac{2}{\rho_i g}\left(\frac{\dot{\epsilon}}{\bar{A}}\right)^{\frac{1}{n}}, \tag{6}$$

where $\bar{A}$ is the depth averaged rheological exponent, n=3 is the rheological exponent, d_w is the water height in the surface crevasse and ρ_0 is the density of surface liquid. The parameter $\dot{\epsilon}$ is the longitudinal strain rate approximated in PSU3D through the isotropic ice divergence

$$\dot{\epsilon} = \left(\frac{\partial u}{\partial x} + \frac{\partial v}{\partial y}\right). \tag{7}$$

BISICLES implements essentially the same criterion, but computes crevasse depths from membrane stresses such that Equations 5-6 become

$$d_s = \frac{\mathrm{tr}(\tau)}{\rho_i g}h + \frac{\rho_w}{\rho_i}d_w, \tag{8}$$

$$d_b = \frac{\rho_i}{\rho_0 - \rho_i}\left(\frac{\mathrm{tr}(\tau)}{\rho_i g}h - h_{ab}\right), \tag{9}$$

where τ is the deviatoric stress tensor, $\mathrm{tr}()$ is the trace operator, and h_{ab} is the thickness above flotation (Sun et al., 2017). In PSU3D ice is calved off when the combined thickness of the surface and bottom crevasses reach at least 75% of the column ice thickness (Pollard et al., 2015), whereas in BISICLES icebergs calve when the sum of the surface and bottom crevasses reaches the distance from ~~sea level to the ice surface~~ ice surface to the waterline.

Water height in surface crevasses (d_w in Equation 5) is computed from biased-corrected CMIP5 model projections to 2300 from the model selection presented in Schannwell et al. (2015). The bias-correction and melt computation approach follows Trusel et al. (2015). In brief, December-January-February (DJF) near-surface temperatures from the CMIP5 ~~Historical~~ historical simulations were compared to high resolution (5.5 km) RACMO2.3 simulations (van Wessem et al., 2016) such that

$$\overline{Bias_{GCM}} = \overline{T_{2m_{GCM}}} - \overline{T_{2m_{RACMO2.3}}}, \tag{10}$$

where $\overline{T_{2m_{GCM}}}$ and $\overline{T_{2m_{RACMO2.3}}}$ are the mean DJF near-surface temperatures over the baseline period 1980-2005 from each GCM and RACMO2.3, respectively. The bias calculation (Equation 10) is restricted to the ice-shelf areas in our two model domains (Figure 1). The best performing GCM (lowest bias) for the RCP4.5 (Figure A1, MIROC-ESM) and RCP8.5 (Figure A2, CSIRO) scenarios were then selected as future forcing.

To convert from near-surface temperature to melt, the empirical formula derived by Trusel et al. (2015) was used. This formula scales surface melt exponentially with mean DJF near-surface temperatures and approximates the surface melt available to fill surface crevasses (R). To compute water height in surface crevasses, d_w is set to (Pollard et al., 2015).

$$d_w = 100R^2. \tag{11}$$

2.3 Model Initialisation

BAS-APISM employs a combined altimetric and velocity initialisation scheme, permitting a steady-state starting condition after initialisation under the assumption that the current ice sheet configuration is close to steady state (Barrand et al., 2013). This is accomplished through the computation of balance fluxes. The motivation for this type of initialisation technique is that the absence of accurate ice thickness datasets leads to the omission of the mechanical model in the cost function employed for the initialisation (Barrand et al., 2013).

BISICLES is initialised by solving an optimisation problem to infer the basal traction coefficient C and the stiffening factor ϕ (also enhancement factor, Equation 1), by matching modelled velocities with observed velocities (Rignot et al., 2011). This type of initialisation is well known and widely employed in ice sheet modelling (MacAyeal, 1992; Cornford et al., 2015). A nonlinear conjugate gradient method was employed to seek a minimum of the objective function

$$J = J_m + J_p \tag{12}$$

where J_m is the misfit between observed and modelled velocities and J_p is a Tikhonov penalty function described by

$$J_p = \lambda_C J_C^{reg} + \lambda_\phi J_\phi^{reg} \tag{13}$$

where λ_C and λ_ϕ are the Tikhonov parameters and J_C^{reg} and J_ϕ^{reg} represent the spatial gradients of C and ϕ integrated over the domain (Cornford et al., 2015). An L-curve analysis was performed to calibrate the Tikhonov parameters and avoid overfitting or overregularisation (Fürst et al., 2015). The selected values are $\lambda_C = 10^{-1}$ and $\lambda_\phi = 10^9$ (Figure A3).

In solving this inverse problem, maps of surface elevation and bedrock topography were taken from the BEDMAP2 (Fretwell et al., 2013) dataset, and a steady state 3-D temperature field was used from a higher order model (Pattyn, 2010). It is only necessary to find solutions with a single sliding law, as the coefficients can be computed from one another to give the same basal traction τ_b, e.g the coefficients for the cases $m = m_1$ and $m = m_2$ must satisfy $C_2|u|^{m_2} = C_1|u|^{m_1}$. We chose $m = 1$ for the inversion simulation.

PSU3D utilises a different algorithm to infer the basal traction coefficient. Instead of matching velocities, the algorithm implemented in PSU3D seeks to minimise the misfit between local surface elevation observations and modelled local surface elevations (Pollard and DeConto, 2012b). To achieve this, the ice-sheet model is run forward in time, and basal traction coefficients are periodically compared and adjusted according to the local surface elevation error. This iterative process is continued until modelled surface elevation converges to the best fit with observed surface elevation (Pollard and DeConto, 2012b). Note that this simpler algorithm does not infer a stiffening factor ϕ for ice shelves. Input maps needed for the inversion algorithm are from ALBMAP (Le Brocq et al., 2010): e.g., ice thickness ~~, bedrock topography, and surface mass balance~~and bedrock topography. For all PSU3D simulations, basal traction fields are interpolated onto the respective model grid from a 5 km Antarctica inversion simulation. The coarser resolution leads to some interpolation artefacts in the basal traction coefficient fields (Figure 2).

2.4 Spin-Up

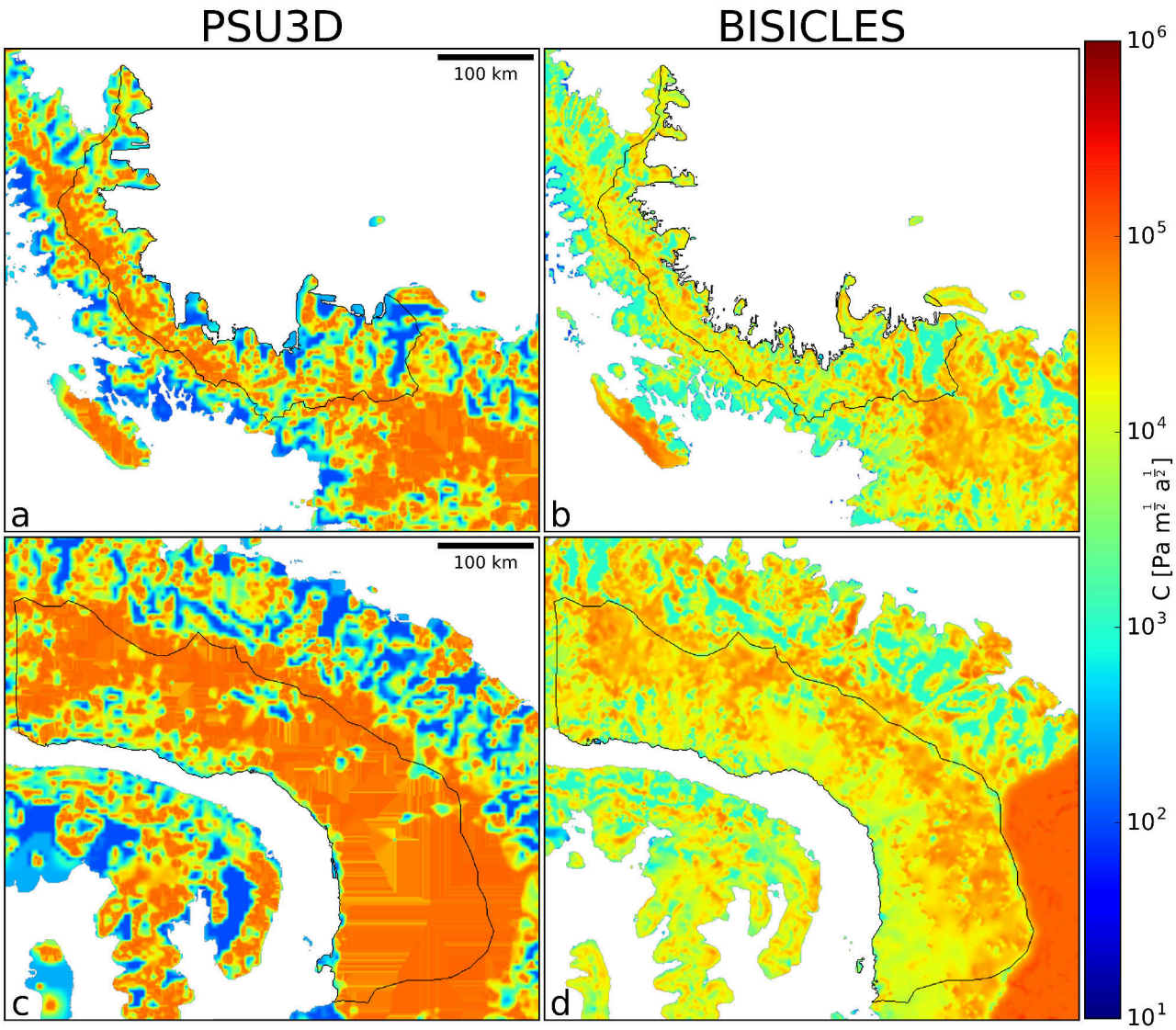

Figure 2. Inferred basal traction fields C for the Larsen C (a,b) and George VI model domains (c,d). Black ~~line denotes~~ lines denote modelled drainage basins.

~~After~~ Following initialisation the sheet-shelf models should be ~~in equilibrium~~ close to equilibrium if the ice sheet is close to steady state, providing $\frac{\partial h}{\partial t} = 0$. However, ~~this~~ owing to data inconsistencies and in part a violation of this steady-state assumption this condition is not fulfilled, requiring a spin-up or relaxation simulation to reach a steady state for each model~~to guarantee a steady-state starting position. To~~ . To tease out the sea-level rise contributions from ice-shelf removal and facilitate comparison across all three ice-sheet models, the employed spin-up approach aims to keep the ice sheet geometry as close as possible to the initial geometry. This is necessary because BAS-APISM provides a stable starting condition after initialisation.

To ensure a minimal change in ice-sheet geometry, we compute a synthetic mass balance (MB) which is simply (Price et al., 2017)

$$MB = FC, \tag{14}$$

where FC is the negative of the modelled thickness field change when the model is run forward a single time step. This synthetic mass balance is applied in all spin-up and perturbation simulations. All simulations are then run forward in time for 50 years with only this forcing applied. To reach steady state, the volume above flotation change with time should be near zero ($\frac{\partial V}{\partial t} \sim 0$) at the end of the spin-up. All of our simulations fulfil this criterion (Figure 3), even though PSU3D simulations are not as close to steady state as BISICLES simulations at the end of the spin-up period.

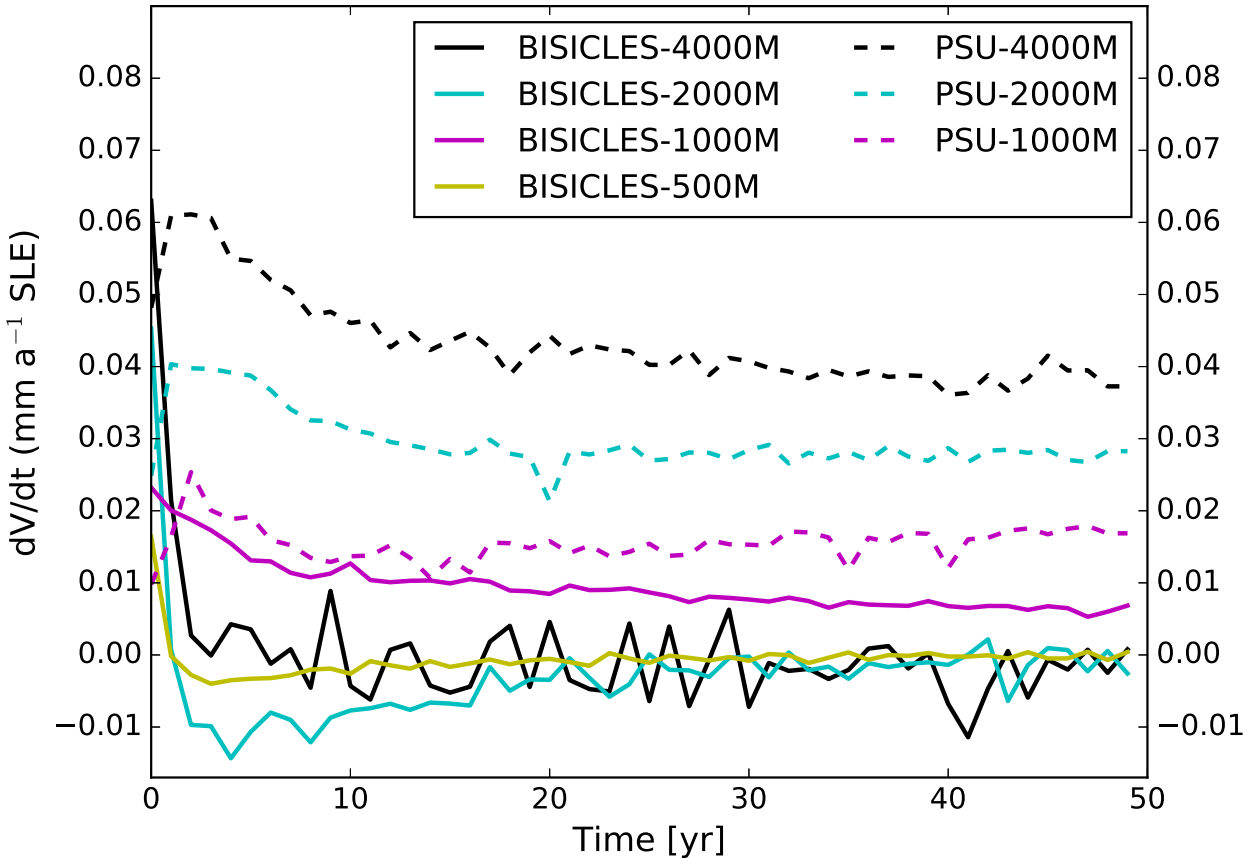

Figure 3. $\frac{\partial V}{\partial t}$ spin-up plot for BISICLES (solid lines) and PSU3D (dashed lines) at different horizontal resolutions.

2.5 Experimental Design

Two sets of experiments were undertaken using the ice-sheet models ~~. In the first simulation (hereafter~~ (Table 1). In Experiment 1~~)~~, immediate ice-shelf collapse was imposed on all three ice-sheet models and combined with a fixed calving front position. This provides an envelope of sea-level rise projections ~~from the best available ice-sheet models~~ for the peninsula region and evaluates the importance of each shelf to the tributary glaciers upstream. Simulations with the sheet-shelf models (PSU3D and BISICLES) were carried out at different horizontal resolutions to investigate the grid dependence on the sea-level rise projections and to select the best compromise between computational demand and appropriate grid resolution (Table 1). In the second simulation (Experiment 2), the two sheet-shelf models (PSU3D and BISICLES) were run at 1 km resolution to simulate ice-shelf retreat and collapse and subsequent tidewater glacier retreat using a physically-based calving relation (Benn et al., 2007; Nick et al., 2010). This relation initiates iceberg calving when the combined depth of surface and bottom crevasses reach a threshold percentage of ice thickness (See Section 2.2). Crevasse depth primarily depends on the stress field of the ice shelf, with extensional stresses providing favourable conditions for crevasse opening, though meltwater hydrofracture may also increase calving rates, a process that has been strongly implicated in the 2002 collapse of Larsen B Ice Shelf (Scambos et al., 2003). In all simulations of Experiment 2 ice-shelf thickness is allowed to evolve freely. This more realistic experiment permits the evaluation of a more gradual loss of buttressing to the upstream glaciers and assesses the effect of a dynamic calving front. In all simulations, perturbations to the surface mass balance are ignored as these are expected to be small in comparison to ice dynamic changes resulting from shelf loss (Barrand et al., 2013). Moreover, ocean melting is set to zero in the perturbation experiments unless stated otherwise.

Table 1. Complete list of all perturbation experiments including sensitivity simulations as well as grid resolutions for Experiments 1 and 2.

Name of experiment	Model	Grid resolution [m]
Experiment 1	BAS-APISM	900
Experiment 1	PSU3D	4000, 2000, 1000
Experiment 1	BISICLES	4000, 2000, 1000, 500
Experiment 1 with linear Weertman	BISICLES	1000
Experiment 1 with cubic Weertman	BISICLES	1000
Experiment 1 with Coulomb sliding	BISICLES	1000
Experiment 1 with bedrock from Huss and Farinotti (2014)	BISICLES	1000
Experiment 2	BISICLES	1000
Experiment 2	PSU3D	1000
Experiment 2 'moderate' ocean melt	PSU3D	1000
Experiment 2 'extreme' ocean melt	PSU3D	1000

3 Results

3.1 Experiment 1: Immediate ice-shelf collapse

Projections of sea-level rise from Larsen C embayment glaciers following immediate shelf collapse (Experiment 1) are small, ranging from 0.5-1.5 mm by 2100 and 0.6-1.6 mm to 2300 (Figure 4a). The sea-level curve rises in the first two decades in

response to loss of backstress provided by the shelf, then decelerates with tributary glaciers adjusting to the new configuration ∼25 years after collapse. Grounding-line retreat of >5 km and extensive dynamic thinning (>0.6 m a^{-1}, propagating ∼75 km inland) is restricted to five outlet glaciers in the southern part of the embayment (Figure 5). In contrast, immediate collapse of George VI Ice Shelf perturbs upstream grounded tributaries by up to 0.8 m a^{-1} averaged over 300 years, and results in 4-11 mm total sea-level rise by 2300 (Figure 4b). The more dramatic response of George VI tributary glaciers means that they have not yet reached steady-state by 2100 (Figure 4d), and PSU3D simulations continue to contribute to sea level well beyond this date. ~~Some of this discrepancy between~~ This discrepancy between the sheet-shelf models ~~is attributed to the fact~~ may be attributed to a combination of differences in initialisation, inferred basal traction fields, and that PSU3D is not as close to steady-state as BISICLES following initialisation and spin-up (Figures 3,A4). Moreover, ice-sheet thinning in response to the collapse event propagates further upstream in PSU3D and is more widespread than in BISICLES, leading to higher rates of mass loss despite similar predicted grounding-line retreat (~~Table ??~~Tables S1,S2). Such a response has been previously attributed to differences in the underlying model physics (L1L2, A-HySSA~~, (Pattyn et al., 2013))~~). Using synthetic geometries, A-HySSA models have shown to be more sensitive to grounding-line advance as well as retreat. These differences are most likely caused by the neglecting of vertical shearing terms in the pure membrane ice-sheet models (Pattyn et al., 2013).

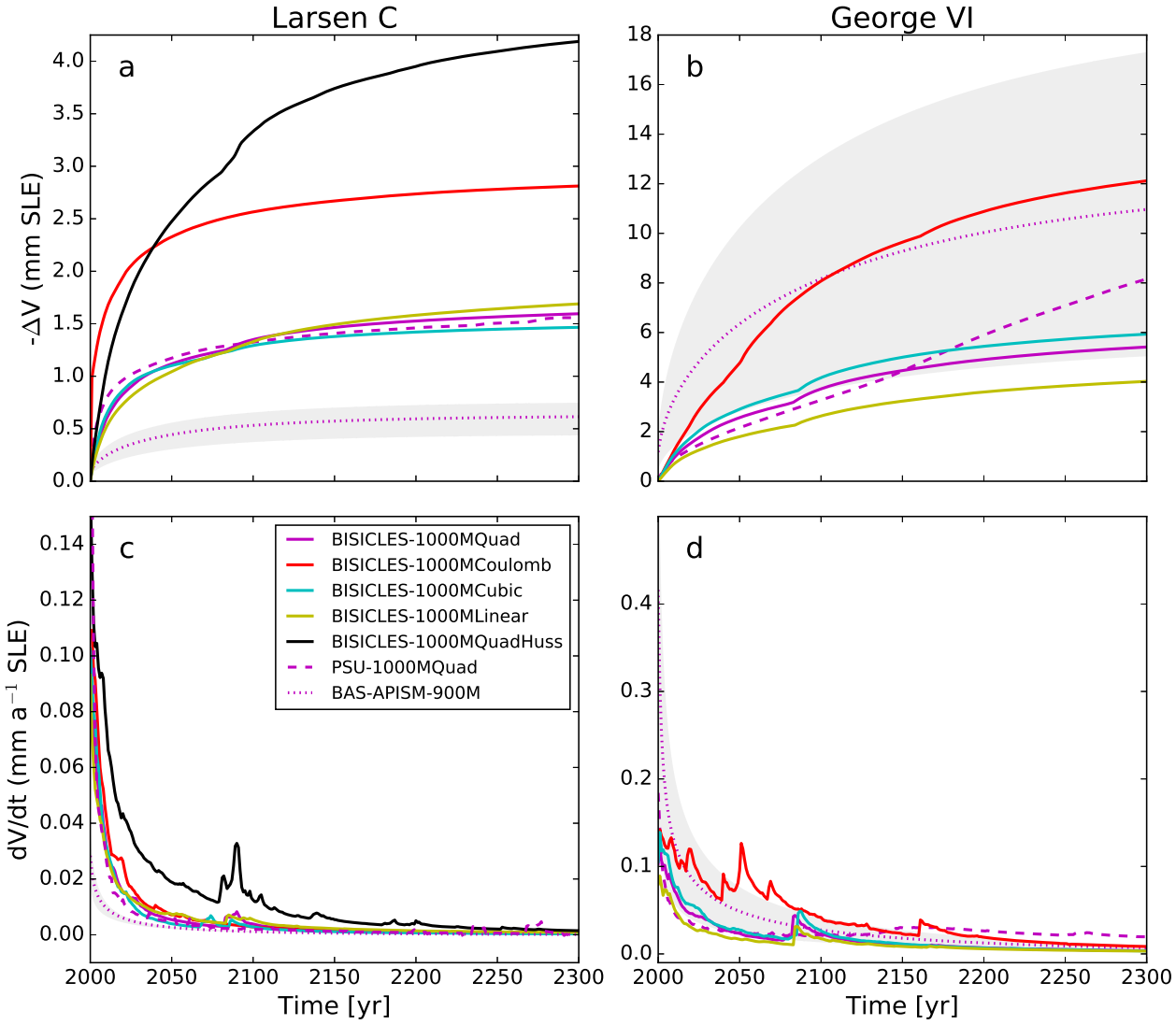

Figure 4. Upper ~~panel~~ panels (a,b) shows SLR projections from Experiment 1 (immediate shelf collapse) for BISICLES (solid lines), PSU3D (dashed lines), and BAS-APISM (dotted line). Lower ~~panel~~ panels (c,d) shows the derivative (rate of change) of the corresponding SLR projections in the upper ~~panel~~ panels (a,b). Grey shading displays uncertainty associated with SLR projections from BAS-APISM. Note different y-axis scales. Projections with Huss and Farinotti (2014) dataset is only available for Larsen C. Quad=Quadratic

While there is a notable grid dependence in BISICLES projections (Figure ~~A4~~A6), this is ~~absent~~ much reduced in the PSU3D projections supporting the findings of previous modelling studies ~~(Pollard and DeConto, 2012a; Pattyn et al., 2013)~~ (Pollard and DeConto, 2012a) that ice-sheet models with the implementation of an internal flux boundary condition are less sensitive to grid resolution. The required first order convergence (Cornford et al., 2016) of the sea-level rise projections in the BISICLES simulations is met for simulations at 1 km and 0.5 km resolution. To facilitate comparison between the two

sheet-shelf models a 1 km grid is employed for Experiment 2.

At 1 km resolution, the combined sea-level rise by 2300 from glaciers in both embayments ranges from 5.6 to 10.4 mm sea-level equivalent, with >60% of the total provided by George VI outlet glaciers. BAS-APISM projects a similar total to 2300 (11.5 mm), though a poor match in simulated spatial patterning of dynamic thinning (Figures 5,6) shows that the simplified model physics and statistical approach to grounding-line retreat do not perform satisfactorily in some areas.

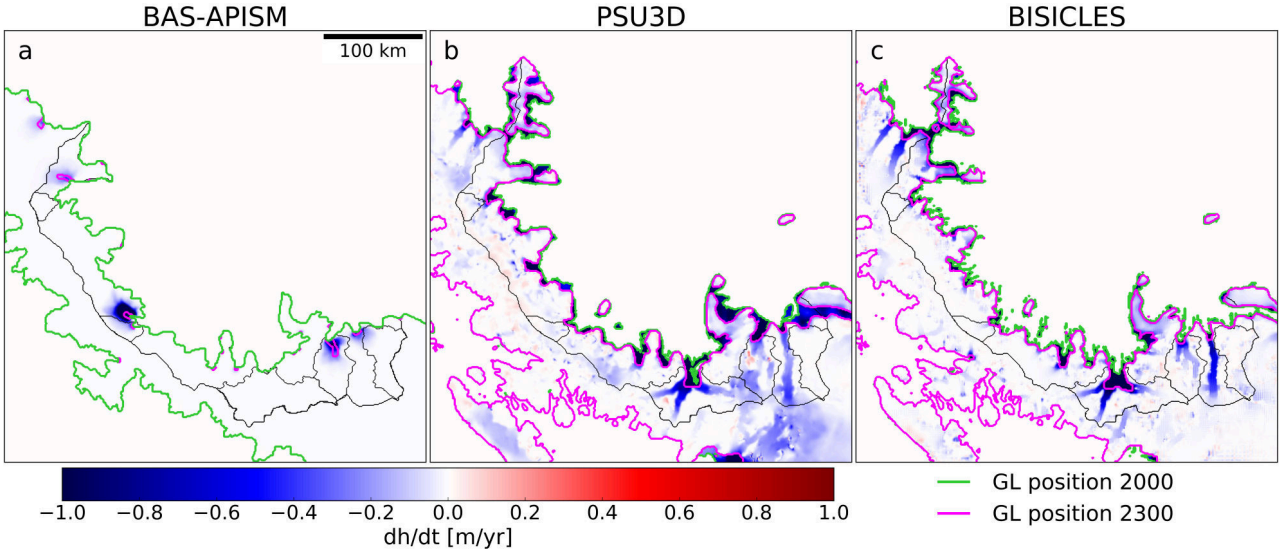

Figure 5. Dynamic thinning (dh/dt) pattern from Experiment 1 (immediate shelf collapse) averaged over the simulation period 2000-2300 for the Larsen C embayment in (a) BAS-APISM, (b) PSU3D, and (c) BISICLES. Black ~~line denotes~~ lines denote modelled drainage basins.

Across all three ice-sheet models, and in both Larsen C and George VI embayment domains, ice-shelf collapse does not result in widespread and extensive grounding-line retreat (Figures 5,6). This was expected for Larsen C outlet glaciers due to a combination of prograde-sloping bedrock topography and the moderate backstress currently provided by the shelf (Fürst et al., 2016). George VI Ice Shelf, however, provides both strong buttressing (Fürst et al., 2016) and mostly marine-based outlet glaciers on retrograde sloping bedrock topography (Figure 1b), conditions expected to be favourable for marine ice sheet instability. Despite this, grounding-line retreat of George VI outlet glaciers is limited to a few locations and <15 km in length (Figure 6). These findings suggest that stabilising forces such as basal and lateral drag may provide enough resistance for the ice sheet in western Palmer Land to remain in a stable configuration following the initial response to ice-shelf collapse. This is supported by earlier modelling studies with idealised geometries, showing that the magnitude of grounding-line retreat is a function of the retrograde sloping channel width (Gudmundsson et al., 2012; Gudmundsson, 2013). The smaller the channel width, the less retreat was simulated (Gudmundsson et al., 2012). Considering the small size of the drainage basins in the peninsula region with channel widths <30 km, the remaining lateral buttressing from shear margins likely impedes any runaway grounding-line retreat.

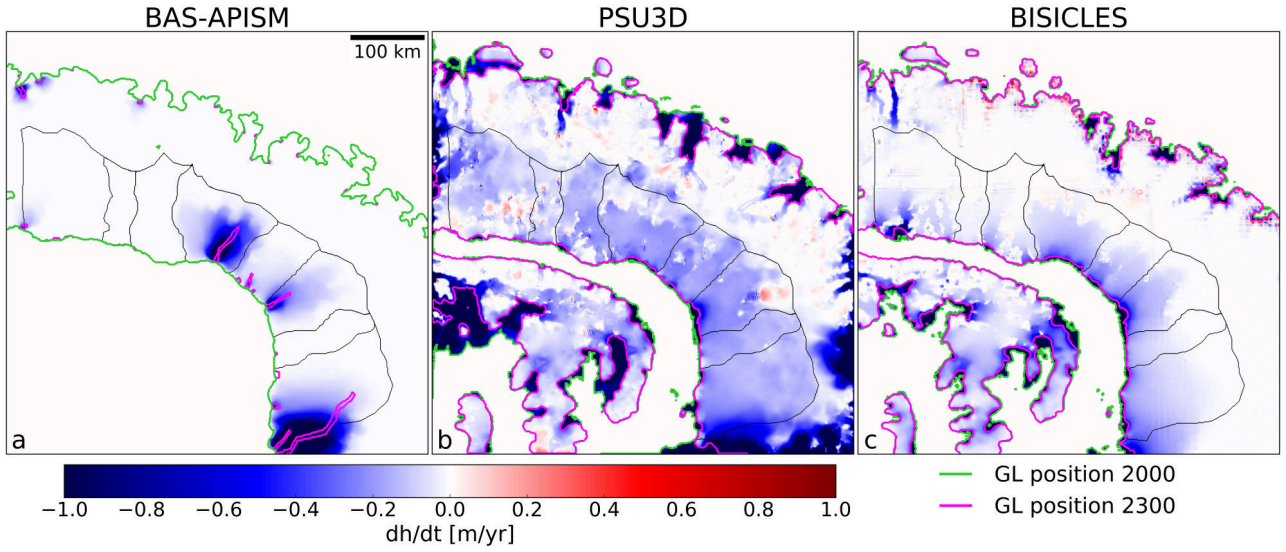

Figure 6. Dynamic thinning (dh/dt) pattern from Experiment 1 (immediate shelf collapse) averaged over the simulation period 2000-2300 for the George VI embayment in (a) BAS-APISM, (b) PSU3D, and (c) BISICLES. Black ~~line denotes~~ lines denote modelled drainage basins.

3.2 Experiment 2: Gradual ice-shelf retreat

When ice-shelf frontal changes are explicitly simulated (Experiment 2) with sheet-shelf models (PSU3D, BISICLES) using a stress-field ~~dependendent~~ dependent calving law, sea-level rise projections span a much larger range. With forcing from the Representative Concentration Pathway (RCP) 8.5 'high emission' scenario, Larsen C and George VI embayment basins combined provide up to 23 mm sea-level equivalent ice loss by 2300 (Figure 7b), with 95% of this total coming from George VI tributary glaciers. The contribution to the sea-level budget from Larsen C embayment glaciers is small (<1.5 mm) and remains equivalent to ~~the fixed calving front simulation, immediate shelf-collapse scenario (Experiment 1).~~ Experiment 1. The sea-level commitment from Larsen C glaciers is modest as complete shelf collapse is not forecast until 2150 in RCP8.5 (Figure 7c), and only 45-60% of the shelf area is lost by 2300 in RCP4.5 ('business-as-usual' scenario). This leads to limited grounding-line retreat and dynamic thinning is restricted to ~~just~~ five outlet glaciers in the southern part of the embayment (Figure 8a). The larger grounded area loss simulated with PSU3D for Larsen C (Figure 7c) is not a response to loss of buttressing force, rather it is due to a more seaward advanced initial grounding-line position introduced in the model spin-up phase, the effect of which on sea-level projections is small (0.28 mm sea-level equivalent).

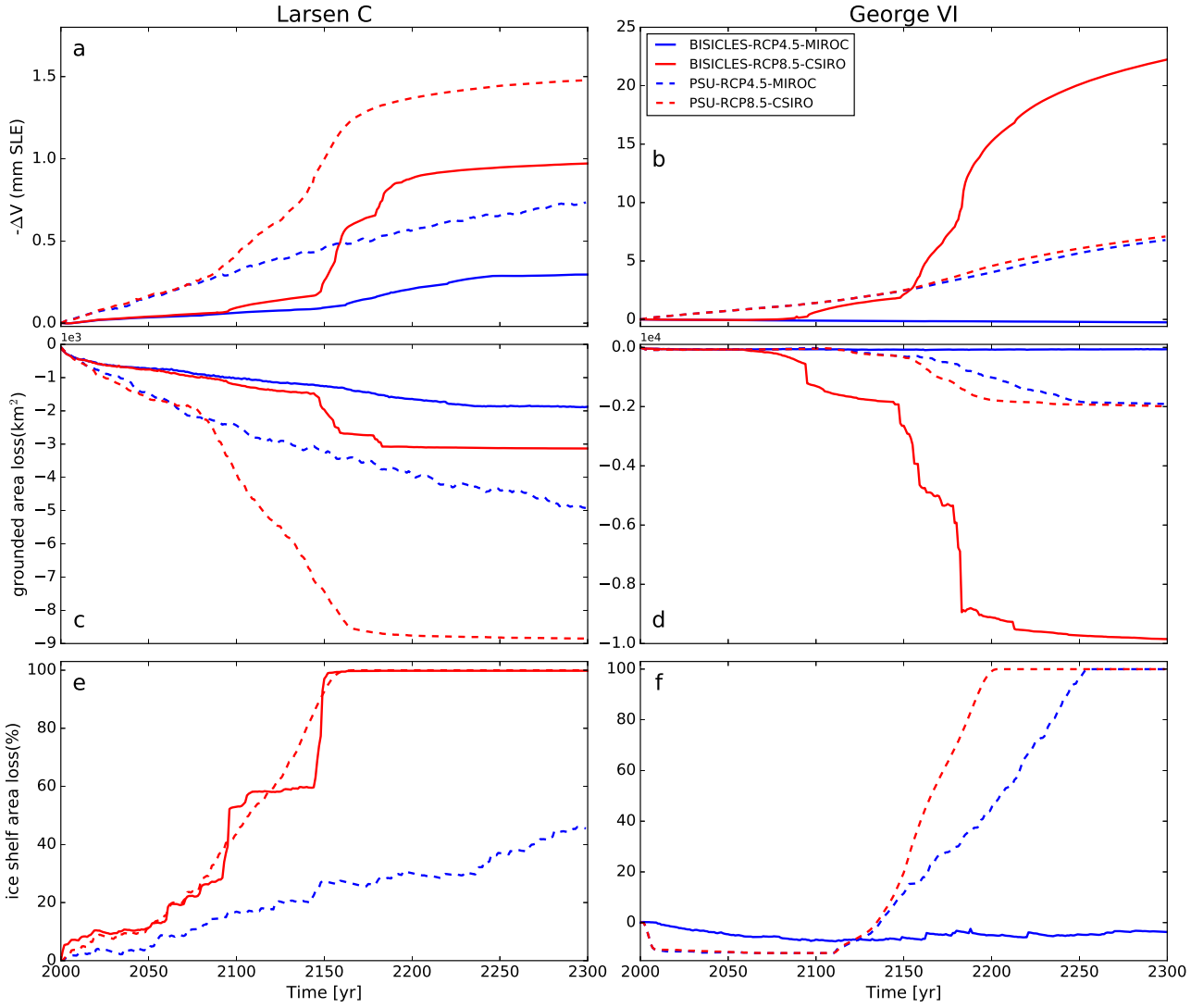

Figure 7. SLR projections from Experiment 2 (dynamic calving front) for Larsen C (a) and George VI ice shelves (b) with corresponding area loss of grounded ice (c,d) and ice shelf area loss (e,f). MIROC and CSIRO denote selected global climate model forcing.

Although projections for Larsen C Ice Shelf glaciers agree reasonably well in absolute numbers across both sheet-shelf models despite differences in their underlying physics, projections diverge for simulations of George VI Ice Shelf glaciers (Figure 7b). Experiment 2 (dynamic calving front) simulations with PSU3D provide very similar sea-level projections to Experiment 1 runs for George VI (immediate ice-shelf collapse; 6.8-7.1 mm from RCP4.5 and 8.5, respectively). In contrast, BISICLES projects ~~no~~ little sea-level rise under RCP4.5 for George VI, as the amount of meltwater available for hydrofracturing is insufficient to initiate ice-shelf collapse or retreat due to the different implementation of the calving law (See Section 2.2). Under RCP8.5, break-up of George VI Ice Shelf occurs at approximately 2100 (Figure 7d), resulting in widespread

grounding-line retreat and sea-level rise of 22 mm by 2300. Both sheet-shelf models project similar sea-level rise ~~by the mid 22nd century in Experiment 2.~~ up to 2150 in Experiment 2 for the George VI domain. In the BISICLES RCP8.5 simulation, however, ~~grounding lines are forced~~ following the collapse of the shelf, calving fronts and grounding lines retreat further back into the marine-based sectors (Figure 8d). ~~This enhanced retreat is absent from Experiment 1 because a fixed calving front is used. In Experiment 2 however, increased~~ After ice-shelf collapse, grounding line and calving front for all drainage basins are almost in identical locations. Increasing rates of calving permit the grounding line to retreat much further inland in the RCP8.5 BISICLES simulation for George VI. As this enhanced grounding-line retreat is only present in Experiment 2, it suggests that this retreat is most likely due to a combination of the dynamic calving front and the marine ice-sheet instability mechanism. Even with a dynamic calving front, enhanced grounding-line retreat for George VI is not triggered before some time after ice-shelf collapse (>15 years, ~~Table ??~~Tables S3,S4), indicating that fast grounding-line retreat is not triggered before the calving front along with the grounding line reaches a retrograde sloping bedrock topography. As a result of widespread grounding-line retreat for George VI in the RCP8.5 scenario (Figure A5), extensive dynamic thinning occurs (>1 m a^{-1}), extending up to 100 km inland in the southern parts of the embayment (Figure 8d). PSU3D simulations do not show enhanced grounding-line retreat in this sector.~~We attribute this to the high levels of basal drag inferred by the inversion procedure~~

We attribute the good agreement across both models for Larsen C to the fact that the area of the marine-based sectors is limited in this domain (2.1 mm contained in marine-based sectors) due to the very mountainous bedrock topography constraining potential grounding-line retreat. This is supported by all simulations across all ice-sheet models as even under a wide range of different forcings the Larsen C embayment does not contribute more than 4.2 mm by 2300. The greater potential to initiate grounding-line retreat is presented by George VI Ice Shelf where much of the ice sheet is marine based with retrograde sloping bedrock topography (Figure ~~2). This higher basal drag prevents outlet glaciers from speeding up enough to cause dynamic thinning such that the glacier fronts reach flotation, thus limiting the extent of deep basal crevasses, which form only in ice close to or at flotation. As a consequence~~ 1b). As this large grounding-line retreat is only initiated in the BISICLES simulation, large differences in sea-level rise projections occur. The most likely scenario for this differing behaviour is due to the difference in the inferred basal traction coefficient fields that affects each model's response to ice-shelf removal. PSU3D ~~never retreats far enough~~ predicts much stickier bedrock conditions in the George VI embayment than BISICLES (Figure 2). These sticky bedrock conditions result in little acceleration of the major outlet glaciers following ice-shelf breakup. This in turn means that the calving law applied to only floating ice cells cannot drive the initial retreat into the marine based sectors as the outlet glaciers do not thin sufficiently to form floating ice tongues. In contrast in the RCP8.5 BISICLES simulation for George VI, speed-up in response to ice-shelf breakup leads to enhanced dynamic thinning of the main outlet glaciers. This thinning in conjunction with the calving law drives the calving front into the marine-based sectors where ~~the marine ice sheet instability could cause further retreat~~further retreat is initiated by a combination of the marine ice-sheet instability and the meltwater driven calving law, resulting in the simulated much higher sea-level rise projections.

3.3 Uncertainty assessment

A range of sensitivity experiments were undertaken to assess the robustness of our model simulations to additional forcings. To assess the impact of an additional ocean forcing, a pair of basal melt anomalies were applied to areas of fully-floating ice in addition to the freely-evolving calving front forcing (Experiment 2). In a first, 'moderate' simulation, the anomaly was set to the current thinning signal of the respective ice shelf (Paolo et al., 2015) for the duration of the forecast period (0.5 m a^{-1} for Larsen C, 1.1 m a^{-1} for George VI). In a second, 'extreme' scenario, the same initial anomaly was applied, then increasing linearly to 3 times the current thinning signal by 2100, remaining at this magnitude to 2300. In each case, sea-level projections with these additional forcings are within 0.2 mm sea-level equivalent of simulations without additional forcings: in other words, it is ice-shelf break-up ~~subject to~~ in combination with the calving criteria that dominates our results. As the basal boundary condition remains poorly constrained in ice-sheet models, yet our model projections show a strong dependence on this condition, Experiment 1 (immediate shelf collapse) was repeated with BISICLES using a range of basal sliding laws. Each of the traditionally-employed power laws result in similar sea-level rise projections to 2300 (1.4-1.6 mm for Larsen C embayment glaciers, and 4-6 mm for George VI glaciers, respectively; Figure 4). Projections to 2300 increase by a factor of two for simulations using a Coulomb-limited sliding law (Tsai et al., 2015), resulting in ~3 mm from Larsen C glaciers and ~12 mm for George VI glaciers. This type of basal sliding law reduces the basal drag in a mobile ~1 km layer which forms immediately upstream of the grounding line, resulting in greater discharge throughout the simulations (~~Table ??~~Tables S3,S4). The importance of better constrained boundary conditions in the peninsula region (bedrock topography and ice thickness) is highlighted by a discrepancy between sea-level rise projections for Larsen C embayment basins using different data products. Although total ice volume and ice volume below sea-level differences between ALBMAP and BEDMAP2 products are small (<15%), a more recent higher-resolution dataset (Huss and Farinotti, 2014) provides an increase of ~100% in ice volume below sea level. When incorporated into ice-sheet model simulations, this boundary condition results in larger grounding-line retreat rates for some basins occupying deeper bedrock troughs. A consequence ~~of this~~ is a sea-level rise projection for Experiment 1 (immediate ice-shelf collapse) with the reference sliding law (Equation 2) that increases by a factor of ~3 (4.2 mm) for the Huss and Farinotti (2014) boundary input dataset, underlining the significance of accurate boundary dataset for sea-level rise projections.

In addition, our experiments show that for simulations of grounding-line motion in response to ice-shelf breakup sheet-shelf models are necessary. The simple model BAS-APISM fails to reproduce the results of the sheet-shelf models due to the simplified physics. Even across sheet-shelf models differences in model physics, model initialisation, calving law implementation and other numerics (e.g. meshing) can lead to substantially different projections under the same forcing (Figure A5). Sea-level rise projections are most sensitive to the choice of sliding law and bedrock geometry. The peninsula is not the only region where these parameters highly affect decadal to centennial sea-level rise projections as similar conclusions were drawn from modelling of outlet glaciers in the Amundsen Sea embayment (Nias et al., 2018). The wide range of sea-level rise responses to different forcing parameters underlines the need for perturbed ensembles to explore key parameter uncertainties (e.g. basal sliding law) for sea-level rise projections in greater detail for the peninsula region. Owing to the increase in computer

power these type of ensemble projections have become feasible at the regional (e.g. Nias et al., 2016) and continental scale (e.g. DeConto and Pollard, 2016).

3.4 Comparison with Larsen B Ice Shelf collapse response

To further assess the impact of ice-shelf break-up, five drainage basins from ~~each ice-shelf embayment~~ the Larsen C embayment (LarI-LarV, Figure 8) and George VI embayment (GeoI-GeoV, Figure 8) were selected for additional analysis. This provides a comparison to real-world examples of the magnitudes and pattern of glacier response to ice-shelf collapse. For Experiment 1 (immediate ice-shelf collapse), the speed up following ice-shelf removal is short lived ($\sim$15 yrs) for both models. Maximum speed-up of $\sim$300% is possible, though the mean maximum speed-up is $\sim$50% (~~Table ??~~Tables S3,S4). These values are smaller than those observed following Larsen B collapse with a maximum of 8fold speed up (Rignot et al., 2004). This may be due to the different areas selected for the speed up calculation. Both rates of ice discharge (mass loss) and grounding-line retreat are greatest immediately following shelf collapse. For 65% of the selected 10 drainage basins, more than 50% of the total modelled grounding-line retreat takes place within 15 years of ice-shelf collapse. Maximum mass loss rates for Larsen C (1.6-5.1 Gt a^{-1}) are smaller than observations for a similar time period for Larsen B (8.0 Gt a^{-1}) (Scambos et al., 2014).

For Experiment 2, total maximum grounding-line retreat rates remain similar for PSU3D in comparison to Experiment 1, while they almost triple for George VI in the BISICLES simulation (21.3 km in Experiment 2, 6.4 km in Experiment 1) in agreement with our computed sea-level rise projections (Figure 7). Due to the gradual loss of buttressing, significant speed up is absent in the years following ice-shelf removal across all basins. The overall dynamic response is less vigorous than in Experiment 1 with the exception of the George VI embayment in the BISICLES simulation where larger grounding-line retreat rates lead to high mass loss rates. However, unlike in Experiment 1, most of the grounding-line retreat and mass loss occur some time after ice-shelf collapse ($>$15 years after ice-shelf removal).

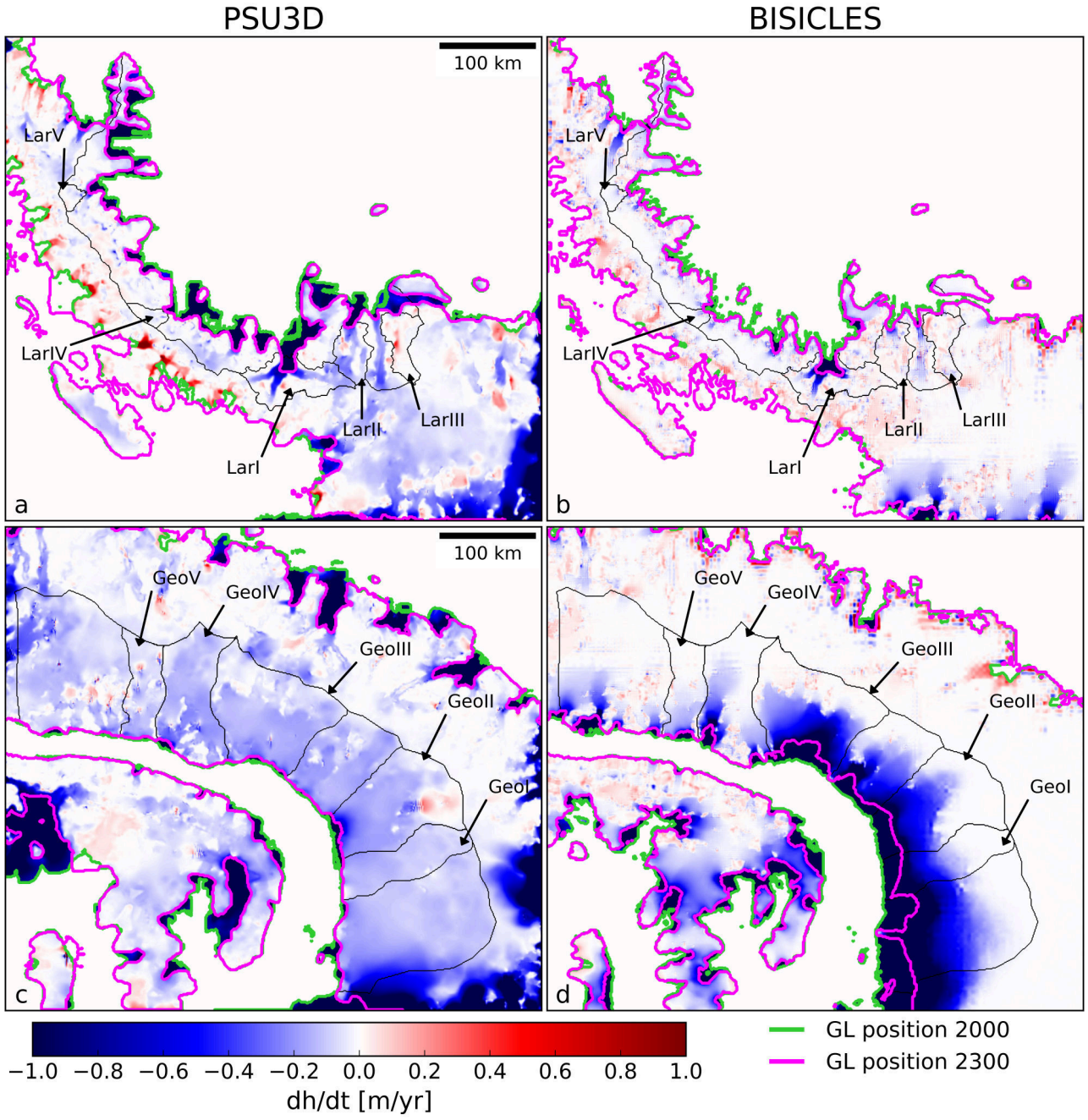

Figure 8. Dynamic thinning (dh/dt pattern from Experiment 2 (dynamic calving front) averaged over the simulation period 2000-2300 in the RCP8.5 scenario for Larsen C (a,c) and George VI embayments (b,d). Black ~~line denotes~~ lines denote modelled drainage basins. LarI-V and GeoI-V indicate drainage basins selected for analysis.

Maximum grounding-line retreat (dGL km), mass change rate (dGt/dt $Gt\ a^{-1}$) and speed up with respect to velocities prior to shelf collapse (dU/dt$_{15}$ unitless) for selected sample basins in Larsen C and George VI embayments for the immediate collapse experiment (Experiment 1). Subscript indicates averaged numbers for the period until 15 years after ice-shelf collapse. For speed up, number in parentheses shows maximum speed up in this time period. Speed up was calculated for a region within five kilometers of the current grounding line in reference to velocities prior to ice-shelf collapse. As BAS-APISM does account for ice-shelf buttressing, speed up calculations were not carried out. Note that grounding-line retreat rates for BAS-APISM are derived from a statistical parameterisation. dGL(dGL$_{15}$) dGt/dt(dGt/dt$_{15}$) dU/dt$_{15}$(dU/dt$_{max}$) dGL(dGL$_{15}$) dGt/dt(dGt/dt$_{15}$) dU/dt$_{15}$(dU/dt$_{max}$) dGL(dGL$_{15}$) dGt/dt(dGt/dt$_{15}$)LarI 21.4(15.2) 0.5(5.1) 40(100)26.8(21.2) 0.3(3.6)1.0(1.8) 0.0(-)0.0(0.0)LarII 7.1(2.3) 0.1(0.7) 1.4(1.7)21.0(11.2) 0.2(0.9)0.7(1.0) 6.3(-)0.2(2.2)LarIII 3.7(0.0) 0.0(0.0) 1.0(1.2)9.7(5.0) 0.0(0.2)0.6(1.0) 1.0(-)0.1(0.9)LarIV 4.3(0.0) 0.0(0.1) 1.2(1.3)5.1(1.3) 0.0(0.0)1.4(1.5) 1.0(-)0.0(0.2)LarV 4.2(1.1) 0.0(0.0) 1.0(1.3)10.0(4.7) 0.0(0.0)2.0(2.9) 0.0(-)0.0(0.0)GeoI 5.6(4.0) 0.3(1.6) 1.2(1.3)5.5(2.1) 0.7(1.8)0.9(1.6) 0.0(-)0.0(0.0)GeoII 10.9(6.4) 0.9(4.2) 1.3(1.4)12.2(6.4) 1.4(4.6)1.0(2.0) 10.5(-)1.0(7.2)GeoIII 8.0(7.0) 0.8(4.0) 1.3(1.4)7.1(5.7) 1.4(5.3)0.8(1.7) 20.8(-)2.3(17.5)GeoIV 7.2(4.9) 0.3(1.2) 1.2(1.4)8.5(5.6) 1.0(3.2)1.3(1.7) 0.0(-)0.0(0.0)GeoV 1.4(1.4) 0.0(0.3) 1.1(1.2)3.1(2.0) 0.3(0.9)1.1(1.5) 0.0(-)0.0(0.0)Maximum grounding-line retreat (dGL km), mass change rate (dGt/dt $Gt\ a^{-1}$) and speed up with respect to velocities prior to shelf collapse (dU/dt$_{15}$ unitless) for selected sample basins in Larsen C and George VI embayments for the dynamic calving front experiment (Experiment 2). Last column presents the same quantities for Experiment 1 for BISICLES using a Coulomb-limited sliding law. Subscript indicates averaged numbers for the period until 15 years after ice-shelf collapse. For speed up, numbers in parentheses show maximum speed up in this time period. Speed up was calculated for a region within five kilometers of the current grounding line. dGL(dGL$_{15}$) dGt/dt(dGt/dt$_{15}$) dU/dt$_{15}$(dU/dt$_{max}$) dGL(dGL$_{15}$) dGt/dt(dGt/dt$_{15}$) dU/dt$_{15}$(dU/dt$_{max}$) dGL(dGL$_{15}$) dGt/dt(dGt/dt$_{15}$) dU/dt$_{15}$(dU/dt$_{max}$)LarI 19.6(3.6) 0.5(2.0) 1.0(1.3)29.4(7.0) 0.3(1.0)1.0(1.0) 14.1(13.7) 0.5(6.4) 0.7(1.1)LarII 2.9(1.3) 0.1(0.4) 1.1(1.3)33.4(6.0) 0.1(0.2)1.0(1.0) 6.8(3.4) 0.2(1.0) 0.8(1.0)LarIII 1.5(0.0) 0.0(0.0) 1.0(1.0)19.3(4.6) 0.1(0.2)0.6(1.0) 0.0(0.0) 0.0(0.0) 1.0(1.0)LarIV 10.7(0.0) 0.0(0.1) 1.0(1.1)10.4(3.8) 0.0(0.0)1.0(1.1) 9.3(1.0) 0.0(0.1) 1.2(1.3)LarV 3.2(0.0) 0.0(0.0) 1.1(1.2)14.6(3.1) 0.0(0.0)1.0(1.0) 3.6(1.0) 0.0(0.0) 1.1(1.2)GeoI 22.3(1.2) 3.3(0.5) 1.0(1.0)4.7(0.0) 0.5(0.6)1.0(1.0) 3.1(3.0) 0.5(1.9) 1.2(1.3)GeoII 23.5(2.7) 4.2(1.7) 0.9(1.0)11.5(1.1) 1.5(2.1)1.0(1.0) 15.8(7.9) 1.9(5.1) 1.3(1.4)GeoIII 25.3(2.1) 5.0(1.3) 1.0(1.0)5.1(0.5) 1.1(1.6)1.0(1.0) 21.9(9.2) 2.3(6.0) 1.3(1.4)GeoIV 25.5(0.0) 1.5(0.2) 1.0(1.4)9.3(1.3) 0.7(0.9)1.0(1.0) 21.0(5.1) 0.7(1.7) 1.2(1.3)GeoV 10.0(1.0) 0.4(0.0) 1.0(1.0)4.3(1.1) 0.2(0.3)1.0(1.0) 9.2(1.1) 0.1(0.3) 1.1(1.2)

4 Conclusions

The most important contributor to the global sea-level budget to 2300 from Antarctic Peninsula ice-shelf-ice sheet dynamics are glaciers in western Palmer Land feeding George VI Ice Shelf. Our envelope of sea-level rise projections ranges from 4-12 mm sea-level equivalent water in Experiment 1, to 6-22 mm sea-level equivalent water in Experiment 2 for George VI. As the highest projection represents only 55% of the grounded ice below sea level in this region (Fretwell et al., 2013), there may yet be even more ice at risk to dynamic mass loss. These projections are relatively insensitive to increased ocean forcing, yet

are highly sensitive to changes in the basal boundary condition and the choice of boundary data set, highlighting the need for improved bed topography data and a more rigorous uncertainty analysis. While Larsen C Ice Shelf's recent calving event may increase its vulnerability ~~of~~ to ice-shelf instability, our simulations under a wide range of future forcing scenarios show that the sea-level commitment of Larsen C embayment glaciers following shelf collapse or retreat are limited to less than ~~4.3~~4.2 mm by 2300 (0.6~~-4.3~~-4.2 mm for Experiment 1; 0.4-1.5 mm for Experiment 2). Individual drainage basin analysis indicates a wide range of responses in response to ice-shelf removal, but overall ice flow speed and mass changes are expected to be of similar magnitude to those observed following the 2002 collapse of Larsen B Ice Shelf.

Appendix A

Competing interests. The authors declare that there are no competing interests.

Acknowledgements. C.S. was supported by a PhD studentship from the University of Birmingham. The computations described in this paper were performed using the University of Birmingham BlueBEAR HPC service, which provides a High Performance Computing service to the University's research community. See http://www.birmingham.ac.uk/bear for more details. We acknowledge the World Climate Research Programmes Working Group on Coupled Modelling, which is responsible for CMIP, and we thank the climate modeling groups for producing and making available their model output (available at http://pcmdi9.llnl.gov/). For CMIP the U.S. Department of Energy's Program for Climate Model Diagnosis and Intercomparison provides coordinating support and led development of software infrastructure in partnership with the Global Organization for Earth System Science Portals. We thank the editor Olivier Gagliardini, Lionel Favier and an anonymous reviewer for comments which improved the manuscript.

References

Arthern, R. J., Hindmarsh, R. C. A., and Williams, C. R.: Flow speed within the Antarctic ice sheet and its controls inferred from satellite observations, Journal of Geophysical Research: Earth Surface, 120, 1171–1188, doi:10.1002/2014JF003239, http://dx.doi.org/10.1002/2014JF003239, 2014JF003239, 2015.

Barrand, N. E., Hindmarsh, R. C. A., Arthern, R. J., Williams, C. R., Mouginot, J., Scheuchl, B., Rignot, E., Ligtenberg, S. R. M., Van Den Broeke, M. R., Edwards, T. L., Cook, A. J., and Simonsen, S. B.: Computing the volume response of the Antarctic Peninsula ice sheet to warming scenarios to 2200, Journal of Glaciology, 59, 397–409, doi:10.3189/2013JoG12J139, http://www.ingentaconnect.com/content/igsoc/jog/2013/00000059/00000215/art00001, 2013.

Benn, D. I., Hulton, N. R. J., and Mottram, R. H.: 'Calving laws', 'sliding laws' and the stability of tidewater glaciers, Annals of Glaciology, 46, 123–130, doi:10.3189/172756407782871161, http://www.ingentaconnect.com/content/igsoc/agl/2007/00000046/00000001/art00019http://dx.doi.org/10.3189/172756407782871161, 2007.

Berger, S., Favier, L., Drews, R., Derwael, J.-J., and Pattyn, F.: The control of an uncharted pinning point on the flow of an Antarctic ice shelf, Journal of Glaciology, 62, 37–45, doi:10.1017/jog.2016.7, 2016.

Borstad, C., Khazendar, A., Scheuchl, B., Morlighem, M., Larour, E., and Rignot, E.: A constitutive framework for predicting weakening and reduced buttressing of ice shelves based on observations of the progressive deterioration of the remnant Larsen B Ice Shelf, Geophysical Research Letters, 43, 2027–2035, doi:10.1002/2015GL067365, http://dx.doi.org/10.1002/2015GL067365, 2016.

Cornford, S. L., Martin, D. F., Graves, D. T., Ranken, D. F., Le Brocq, A. M., Gladstone, R. M., Payne, A. J., Ng, E. G., and Lipscomb, W. H.: Adaptive mesh, finite volume modeling of marine ice sheets, Journal of Computational Physics, 232, 529–549, doi:10.1016/j.jcp.2012.08.037, http://www.sciencedirect.com/science/article/pii/S0021999112005050, 2013.

Cornford, S. L., Martin, D. F., Payne, A. J., Ng, E. G., Le Brocq, A. M., Gladstone, R. M., Edwards, T. L., Shannon, S. R., Agosta, C., van den Broeke, M. R., Hellmer, H. H., Krinner, G., Ligtenberg, S. R. M., Timmermann, R., and Vaughan, D. G.: Century-scale simulations of the response of the West Antarctic Ice Sheet to a warming climate, The Cryosphere, 9, 1579–1600, doi:10.5194/tc-9-1579-2015, http://www.the-cryosphere.net/9/1579/2015/, 2015.

Cornford, S. L., Martin, D. F., Lee, V., Payne, A. J., and Ng, E. G.: Adaptive mesh refinement versus subgrid friction interpolation in simulations of Antarctic ice dynamics, Annals of Glaciology, 57, 1–9, doi:10.1017/aog.2016.13, http://dx.doi.org/10.1017/aog.2016.13, 2016.

DeConto, R. M. and Pollard, D.: Contribution of Antarctica to past and future sea-level rise, Nature, 531, 591–597, doi:10.1038/nature17145, http://dx.doi.org/10.1038/nature17145, 2016.

Fretwell, P., Pritchard, H. D., Vaughan, D. G., Bamber, J. L., Barrand, N. E., Bell, R., Bianchi, C., Bingham, R. G., Blankenship, D. D., Casassa, G., Catania, G., Callens, D., Conway, H., Cook, A. J., Corr, H. F. J., Damaske, D., Damm, V., Ferraccioli, F., Forsberg, R., Fujita, S., Gim, Y., Gogineni, P., Griggs, J. A., Hindmarsh, R. C. A., Holmlund, P., Holt, J. W., Jacobel, R. W., Jenkins, A., Jokat, W., Jordan, T., King, E. C., Kohler, J., Krabill, W., Riger-Kusk, M., Langley, K. A., Leitchenkov, G., Leuschen, C., Luyendyk, B. P., Matsuoka, K., Mouginot, J., Nitsche, F. O., Nogi, Y., Nost, O. A., Popov, S. V., Rignot, E., Rippin, D. M., Rivera, A., Roberts, J., Ross, N., Siegert, M. J., Smith, A. M., Steinhage, D., Studinger, M., Sun, B., Tinto, B. K., Welch, B. C., Wilson, D., Young, D. A., Xiangbin, C., and Zirizzotti, A.: Bedmap2: Improved ice bed, surface and thickness datasets for Antarctica, The Cryosphere, 7, 375–393, doi:10.5194/tc-7-375-2013, http://www.the-cryosphere.net/7/375/2013/, 2013.

Fürst, J. J., Durand, G., Gillet-Chaulet, F., Merino, N., Tavard, L., Mouginot, J., Gourmelen, N., and Gagliardini, O.: Assimilation of Antarctic velocity observations provides evidence for uncharted pinning points, The Cryosphere, 9, 1427–1443, doi:10.5194/tc-9-1427-2015, http://www.the-cryosphere.net/9/1427/2015/, 2015.

Fürst, J. J., Durand, G., Gillet-Chaulet, F., Tavard, L., Rankl, M., Braun, M., and Gagliardini, O.: The safety band of Antarctic ice shelves, Nature Clim. Change, 6, 479–482, doi:10.1038/nclimate2912, http://dx.doi.org/10.1038/nclimate2912, 2016.

Gudmundsson, G. H.: Ice-shelf buttressing and the stability of marine ice sheets, The Cryosphere, 7, 647–655, doi:10.5194/tc-7-647-2013, http://www.the-cryosphere.net/7/647/2013/, 2013.

Gudmundsson, G. H., Krug, J., Durand, G., Favier, L., and Gagliardini, O.: The stability of grounding lines on retrograde slopes, The Cryosphere, 6, 1497–1505, doi:10.5194/tc-6-1497-2012, http://www.the-cryosphere.net/6/1497/2012/, 2012.

Hindmarsh, R. C. A.: A numerical comparison of approximations to the Stokes equations used in ice sheet and glacier modeling, Journal of Geophysical Research: Earth Surface, 109, n/a–n/a, doi:10.1029/2003JF000065, http://dx.doi.org/10.1029/2003JF000065, 2004.

Hogg, A. E., Shepherd, A., Cornford, S. L., Briggs, K. H., Gourmelen, N., Graham, J. A., Joughin, I., Mouginot, J., Nagler, T., Payne, A. J., Rignot, E., and Wuite, J.: Increased ice flow in Western Palmer Land linked to ocean melting, Geophysical Research Letters, 44, 4159–4167, doi:10.1002/2016GL072110, http://dx.doi.org/10.1002/2016GL072110, 2017.

Holland, P. R., Brisbourne, A., Corr, H. F. J., McGrath, D., Purdon, K., Paden, J., Fricker, H. A., Paolo, F. S., and Fleming, A. H.: Oceanic and atmospheric forcing of Larsen C Ice-Shelf thinning, The Cryosphere, 9, 1005–1024, doi:10.5194/tc-9-1005-2015, http://www.the-cryosphere.net/9/1005/2015/, 2015.

Huss, M. and Farinotti, D.: A high-resolution bedrock map for the Antarctic Peninsula, The Cryosphere, 8, 1261–1273, doi:10.5194/tc-8-1261-2014, http://www.the-cryosphere.net/8/1261/2014/, 2014.

Hutter, K.: Theoretical glaciology: Material science of ice and the mechanics of glaciers and ice sheets, vol. 1, Springer, 1983.

Jansen, D., Luckman, A. J., Cook, A., Bevan, S., Kulessa, B., Hubbard, B., and Holland, P. R.: Brief Communication: Newly developing rift in Larsen C Ice Shelf presents significant risk to stability, The Cryosphere, 9, 1223–1227, doi:10.5194/tc-9-1223-2015, http://www.the-cryosphere.net/9/1223/2015/, 2015.

Kulessa, B., Jansen, D., Luckman, A. J., King, E. C., and Sammonds, P. R.: Marine ice regulates the future stability of a large Antarctic ice shelf, Nat Commun, 5, 3707, doi:10.1038/ncomms4707, http://dx.doi.org/10.1038/ncomms4707, 2014.

Le Brocq, A. M., Payne, A. J., and Vieli, A.: An improved Antarctic dataset for high resolution numerical ice sheet models (ALBMAP v1), Earth System Science Data, 2, 247–260, doi:10.5194/essd-2-247-2010, http://www.earth-syst-sci-data.net/2/247/2010/, 2010.

MacAyeal, D. R.: The basal stress distribution of Ice Stream E, Antarctica, inferred by control methods, Journal of Geophysical Research: Solid Earth, 97, 595–603, doi:10.1029/91JB02454, http://dx.doi.org/10.1029/91JB02454, 1992.

Martín-Español, A., Zammit-Mangion, A., Clarke, P. J., Flament, T., Helm, V., King, M. A., Luthcke, S. B., Petrie, E., Rémy, F., Schön, N., Wouters, B., and Bamber, J. L.: Spatial and temporal Antarctic Ice Sheet mass trends, glacio-isostatic adjustment, and surface processes from a joint inversion of satellite altimeter, gravity, and GPS data, Journal of Geophysical Research: Earth Surface, 121, 182–200, doi:10.1002/2015JF003550, http://dx.doi.org/10.1002/2015JF003550, 2016.

McMillan, M., Shepherd, A., Sundal, A., Briggs, K., Muir, A., Ridout, A., Hogg, A., and Wingham, D.: Increased ice losses from Antarctica detected by CryoSat-2, Geophysical Research Letters, 41, 3899–3905, doi:10.1002/2014GL060111, http://dx.doi.org/10.1002/2014GL060111, 2014.

Mercer, J. H.: West Antarctic ice sheet and CO2 greenhouse effect: A threat of disaster, Nature, 271, 321–325, doi:10.1038/271321a0, http://dx.doi.org/10.1038/271321a0, 1978.

Morris, E. M. and Vaughan, D. G.: Spatial and temporal variation of surface temperature on the Antarctic Peninsula and the limit of viability of ice shelves, in: Antarctic Peninsula Climate Variability: Historical and Paleoenvironmental Perspectives, pp. 61–68, American Geophysical Union, doi:10.1029/AR079p0061, http://dx.doi.org/10.1029/AR079p0061, 2003.

Nias, I. J., Cornford, S. L., and Payne, A. J.: Contrasting the modelled sensitivity of the Amundsen Sea Embayment ice streams, Journal of Glaciology, 62, 552–562, doi:10.1017/jog.2016.40, 2016.

Nias, I. J., Cornford, S. L., and Payne, A. J.: New Mass-Conserving Bedrock Topography for Pine Island Glacier Impacts Simulated Decadal Rates of Mass Loss, Geophysical Research Letters, 0, doi:10.1002/2017GL076493, 2018.

Nick, F. M., van der Veen, C. J., Vieli, A., and Benn, D. I.: A physically based calving model applied to marine outlet glaciers and implications for the glacier dynamics, Journal of Glaciology, 56, 781–794, doi:10.3189/002214310794457344, http://dx.doi.org/10.3189/002214310794457344, 2010.

Paolo, F. S., Fricker, H. A., and Padman, L.: Volume loss from Antarctic ice shelves is accelerating, Science, 348, 327–331, doi:10.1126/science.aaa0940, http://dx.doi.org/10.1126/science.aaa0940, 2015.

Pattyn, F.: Antarctic subglacial conditions inferred from a hybrid ice sheet/ice stream model, Earth and Planetary Science Letters, 295, 451–461, doi:10.1016/j.epsl.2010.04.025, http://www.sciencedirect.com/science/article/pii/S0012821X10002712, 2010.

Pattyn, F. and Durand, G.: Why marine ice sheet model predictions may diverge in estimating future sea level rise, Geophysical Research Letters, 40, 4316–4320, doi:10.1002/grl.50824, http://dx.doi.org/10.1002/grl.50824, 2013.

Pattyn, F., Perichon, L., Durand, G., Favier, L., Gagliardini, O., Hindmarsh, R. C. A., Zwinger, T., Albrecht, T., Cornford, S., Docquier, D., Fürst, J. J., Goldberg, D., Gudmundsson, G. H., Humbert, A., Hütten, M., Huybrechts, P., Jouvet, G., Kleiner, T., Larour, E., Martin, D., Morlighem, M., Payne, A. J., Pollard, D., Rückamp, M., Rybak, O., Seroussi, H., Thoma, M., and Wilkens, N.: Grounding-line migration in plan-view marine ice-sheet models: Results of the ice2sea MISMIP3d intercomparison, Journal of Glaciology, 59, 410–422, doi:10.3189/2013JoG12J129, http://www.ingentaconnect.com/content/igsoc/jog/2013/00000059/00000215/art00002, 2013.

Pollard, D. and DeConto, R. M.: Description of a hybrid ice sheet-shelf model, and application to Antarctica, Geosci. Model Dev., 5, 1273–1295, doi:10.5194/gmd-5-1273-2012, http://www.geosci-model-dev.net/5/1273/2012/, 2012a.

Pollard, D. and DeConto, R. M.: A simple inverse method for the distribution of basal sliding coefficients under ice sheets, applied to Antarctica, The Cryosphere, 6, 953–971, doi:10.5194/tc-6-953-2012, http://www.the-cryosphere.net/6/953/2012/, 2012b.

Pollard, D., DeConto, R. M., and Alley, R. B.: Potential Antarctic Ice Sheet retreat driven by hydrofracturing and ice cliff failure, Earth and Planetary Science Letters, 412, 112–121, doi:10.1016/j.epsl.2014.12.035, http://www.sciencedirect.com/science/article/pii/S0012821X14007961, 2015.

Price, S. F., Hoffman, M. J., Bonin, J. A., Howat, I. M., Neumann, T., Saba, J., Tezaur, I., Guerber, J., Chambers, D. P., Evans, K. J., Kennedy, J. H., Lenaerts, J., Lipscomb, W. H., Perego, M., Salinger, A. G., Tuminaro, R. S., van den Broeke, M. R., and Nowicki, S. M. J.: An ice sheet model validation framework for the Greenland ice sheet, Geoscientific Model Development, 10, 255–270, doi:10.5194/gmd-10-255-2017, http://www.geosci-model-dev.net/10/255/2017/, 2017.

Rignot, E., Casassa, G., Gogineni, P., Krabill, W., Rivera, A., and Thomas, R.: Accelerated ice discharge from the Antarctic Peninsula following the collapse of Larsen B Ice Shelf, Geophysical Research Letters, 31, L18 401, doi:10.1029/2004GL020697, http://dx.doi.org/10.1029/2004GL020697, 2004.

Rignot, E., Mouginot, J., and Scheuchl, B.: Ice Flow of the Antarctic Ice Sheet, Science, 333, 1427–1430, doi:10.1126/science.1208336, http://science.sciencemag.org/sci/333/6048/1427.full.pdf, 2011.

Scambos, T., Hulbe, C., and Fahnestock, M.: Climate-induced ice shelf disintegration in the Antarctic Peninsula, in: Antarctic Peninsula Climate Variability: Historical and Paleoenvironmental Perspectives, pp. 79–92, American Geophysical Union, doi:10.1029/AR079p0079, http://dx.doi.org/10.1029/AR079p0079, 2003.

Scambos, T. A., Berthier, E., Haran, T., Shuman, C. A., Cook, A. J., Ligtenberg, S. R. M., and Bohlander, J.: Detailed ice loss pattern in the northern Antarctic Peninsula: Widespread decline driven by ice front retreats, The Cryosphere, 8, 2135–2145, doi:10.5194/tc-8-2135-2014, http://www.the-cryosphere.net/8/2135/2014/, 2014.

Schannwell, C., Barrand, N. E., and Radić, V.: Modeling ice dynamic contributions to sea level rise from the Antarctic Peninsula, Journal of Geophysical Research: Earth Surface, 120, 2374–2392, doi:10.1002/2015JF003667, http://dx.doi.org/10.1002/2015JF003667, 2015.

Schannwell, C., Barrand, N. E., and Radić, V.: Future sea-level rise from tidewater and ice-shelf tributary glaciers of the Antarctic Peninsula, Earth and Planetary Science Letters, 453, 161–170, doi:10.1016/j.epsl.2016.07.054, http://www.sciencedirect.com/science/article/pii/S0012821X16304101, 2016.

Schoof, C.: Ice sheet grounding line dynamics: Steady states, stability, and hysteresis, Journal of Geophysical Research, 112, F03S28, doi:10.1029/2006JF000664, http://dx.doi.org/10.1029/2006JF000664, 2007.

Sun, S., Cornford, S., Gladstone, R., Zhao, L., and Moore, J.: Ice shelf fracture parameterization in an ice sheet model, The Cryosphere Discussions, 2017, 1–23, doi:10.5194/tc-2017-53, http://www.the-cryosphere-discuss.net/tc-2017-53/, 2017.

Trusel, L. D., Frey, K. E., Das, S. B., Karnauskas, K. B., Kuipers Munneke, P., van Meijgaard, E., and van den Broeke, M. R.: Divergent trajectories of Antarctic surface melt under two twenty-first-century climate scenarios, Nature Geosci, 8, 927–932, doi:10.1038/ngeo2563, http://dx.doi.org/10.1038/ngeo2563, 2015.

Tsai, V. C., Stewart, A. L., and Thompson, A. F.: Marine ice-sheet profiles and stability under Coulomb basal conditions, Journal of Glaciology, 61, 205–215, doi:10.3189/2015JoG14J221, http://www.ingentaconnect.com/content/igsoc/jog/2015/00000061/00000226/art00001, 2015.

van Wessem, J. M., Ligtenberg, S. R. M., Reijmer, C. H., van de Berg, W. J., van den Broeke, M. R., Barrand, N. E., Thomas, E. R., Turner, J., Wuite, J., Scambos, T. A., and van Meijgaard, E.: The modelled surface mass balance of the Antarctic Peninsula at 5.5 km horizontal resolution, The Cryosphere, 10, 271–285, doi:10.5194/tc-10-271-2016, http://dx.doi.org/10.5194/tc-10-271-2016, 2016.

Vaughan, D., Marshall, G., Connolley, W., Parkinson, C., Mulvaney, R., Hodgson, D., King, J., Pudsey, C., and Turner, J.: Recent Rapid Regional Climate Warming on the Antarctic Peninsula, Climatic Change, 60, 243–274, doi:10.1023/A:1026021217991, http://dx.doi.org/10.1023/A:1026021217991, 2003.

Wouters, B., Martín-Español, A., Helm, V., Flament, T., van Wessem, J. M., Ligtenberg, S. R. M., van den Broeke, M. R., and Bamber, J. L.: Dynamic thinning of glaciers on the Southern Antarctic Peninsula, Science, 348, 899–903, doi:10.1126/science.aaa5727, http://www.sciencemag.org/content/348/6237/899.abstract, 2015.

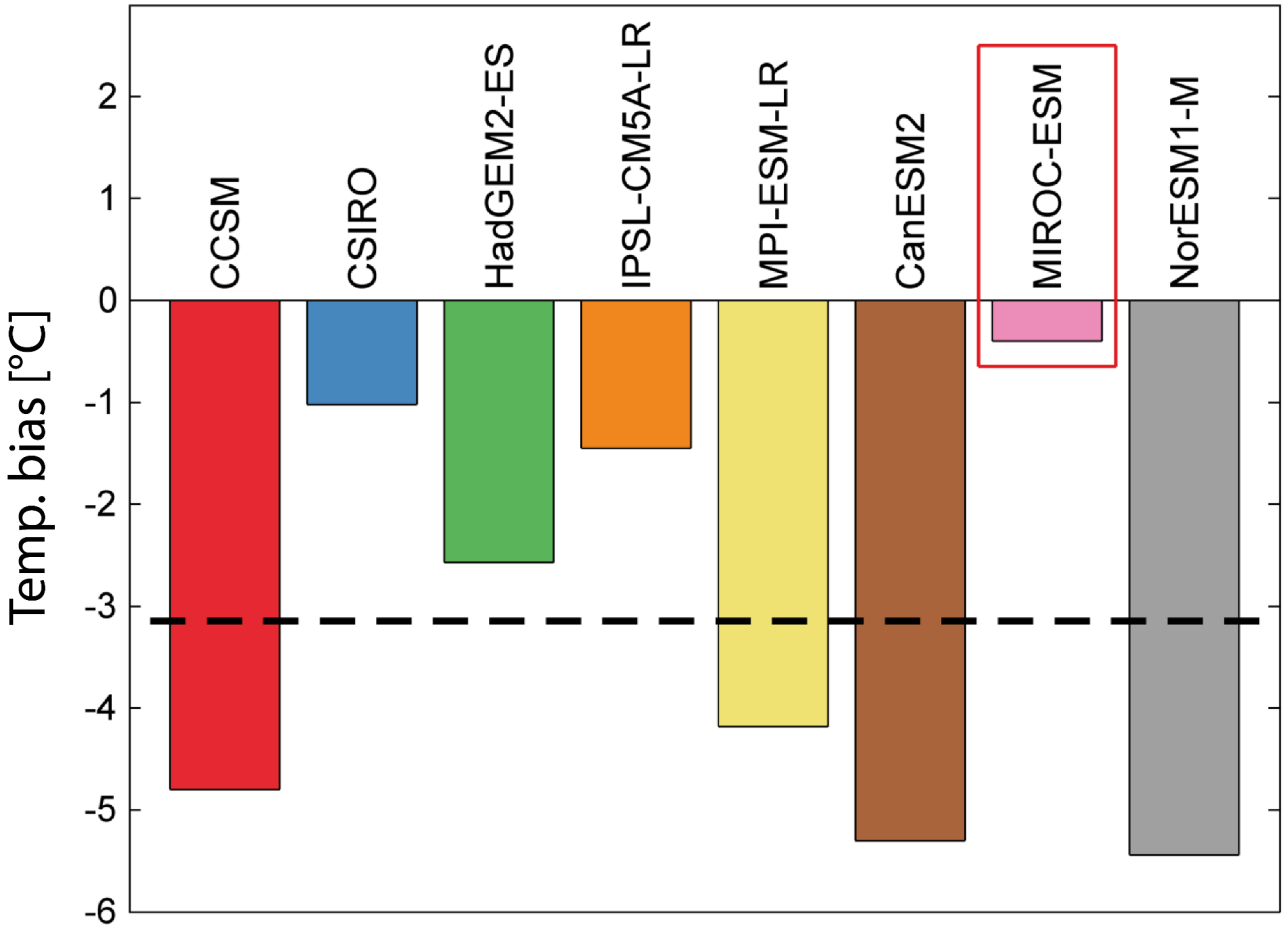

Figure A1. Near-surface temperature bias for the baseline period 1980-2005 in GCMs for RCP4.5 projections in relation to ERA-Interim. Dashed black line indicates multi-model mean (-3.1±2.0°C). The selected forcing is highlighted by the red box.

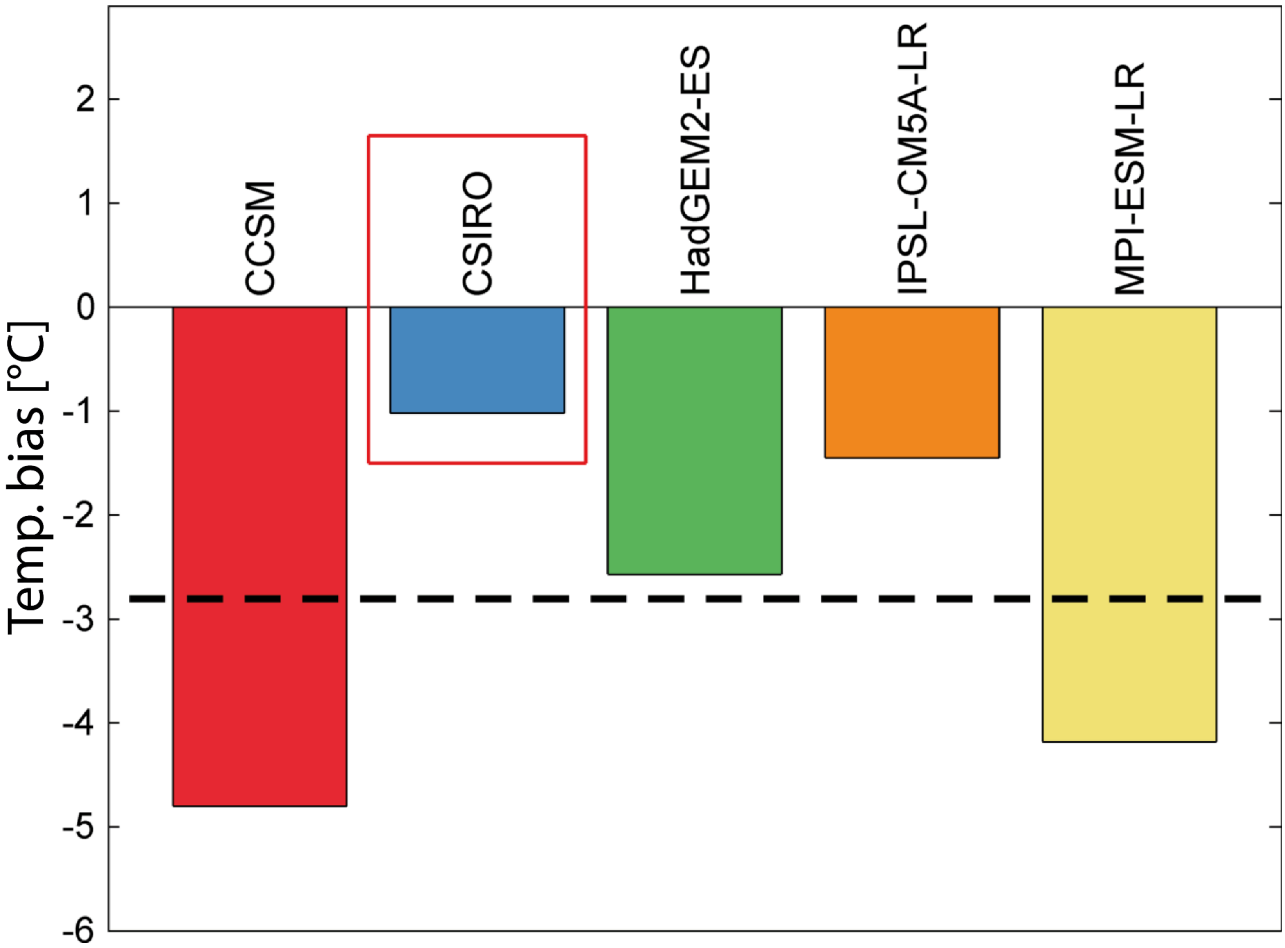

Figure A2. Near-surface temperature bias for the baseline period 1980-2005 in GCMs for RCP8.5 projections in relation to ERA-Interim. Dashed black line indicates multi-model mean (-2.8±1.7°C). The selected forcing is highlighted by the red box.

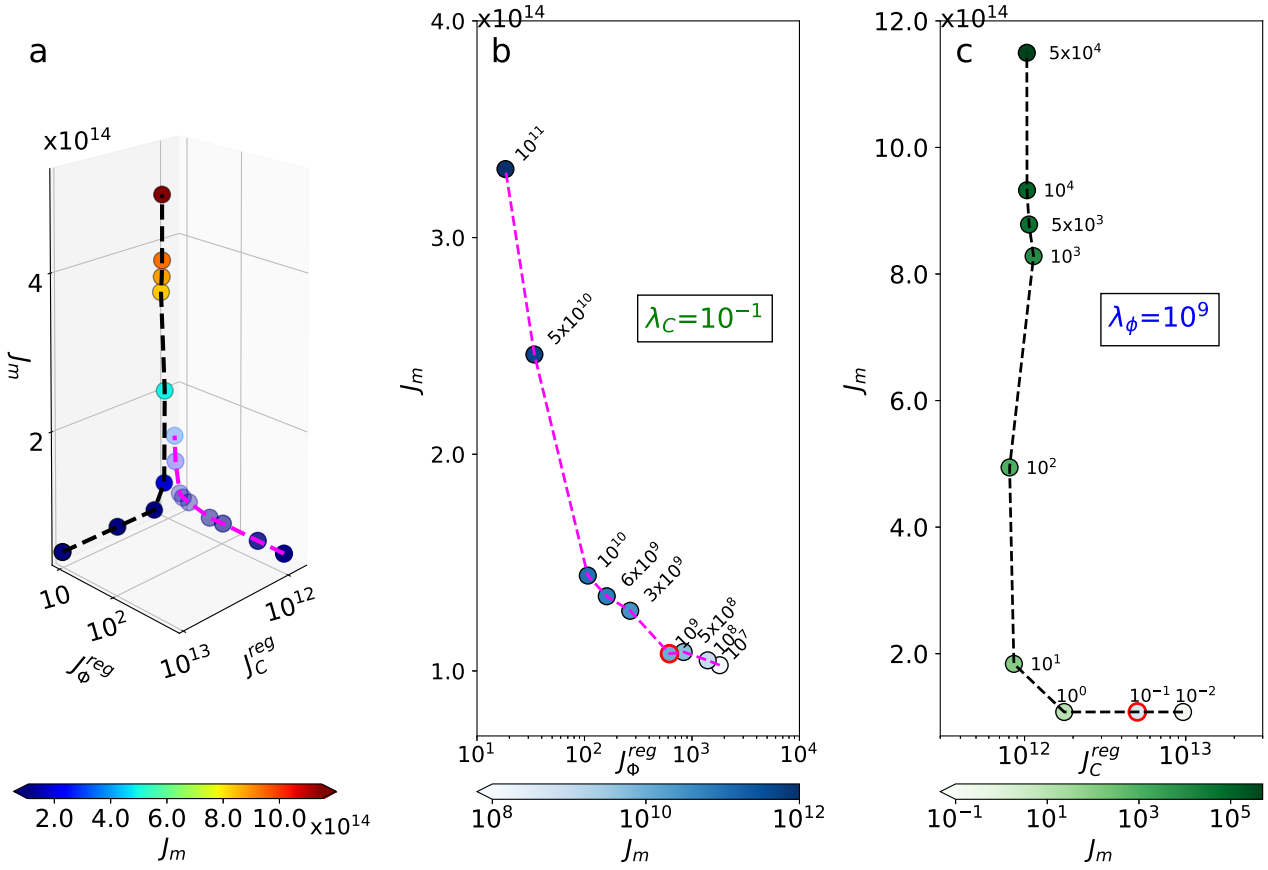

Figure A3. BISICLES L-curve analysis to select Tikhonov parameters λ_ϕ and λ_C: (a) 3-D scatter plot of the model-data misfit J_m as a function of the regularisation terms J_C^{reg} and J_ϕ^{reg}. (b) 2-D cross section for variable λ_ϕ and λ_C fixed at 10^{-1} Pa^{-2} m^6 a^{-4}. (c) Reverse case with constant λ_ϕ at 10^9 m^4 a^{-2} and λ_C varying. The units of J_m and J_C^{reg} are m^4 a^{-2} and Pa^2 m^{-2} a^2, respectively. J_ϕ^{reg} is unitless. Selected values are highlighted by red circles in (b) and (c). The layout was inspired by Berger et al. (2016).

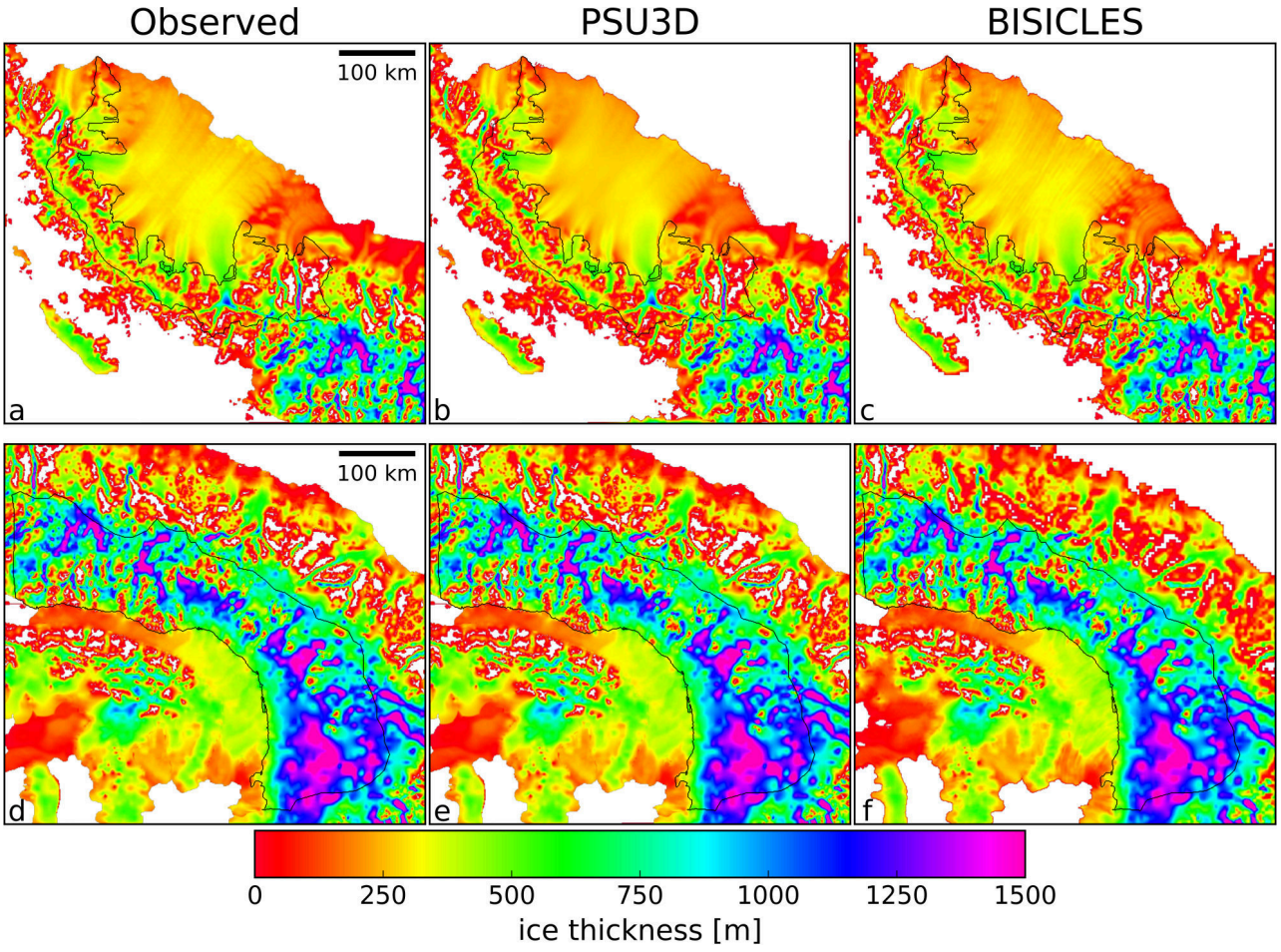

Figure A4. Observed ice thickness distribtution (BEDMAP2(Fretwell et al., 2013)) for Larsen C (a) and George VI (d) embayments and modelled ice thickness distribution after spin-up for Larsen C (b,c) and George VI (e,f) embayments. Black ~~line denotes~~ lines denote modelled drainage basins.

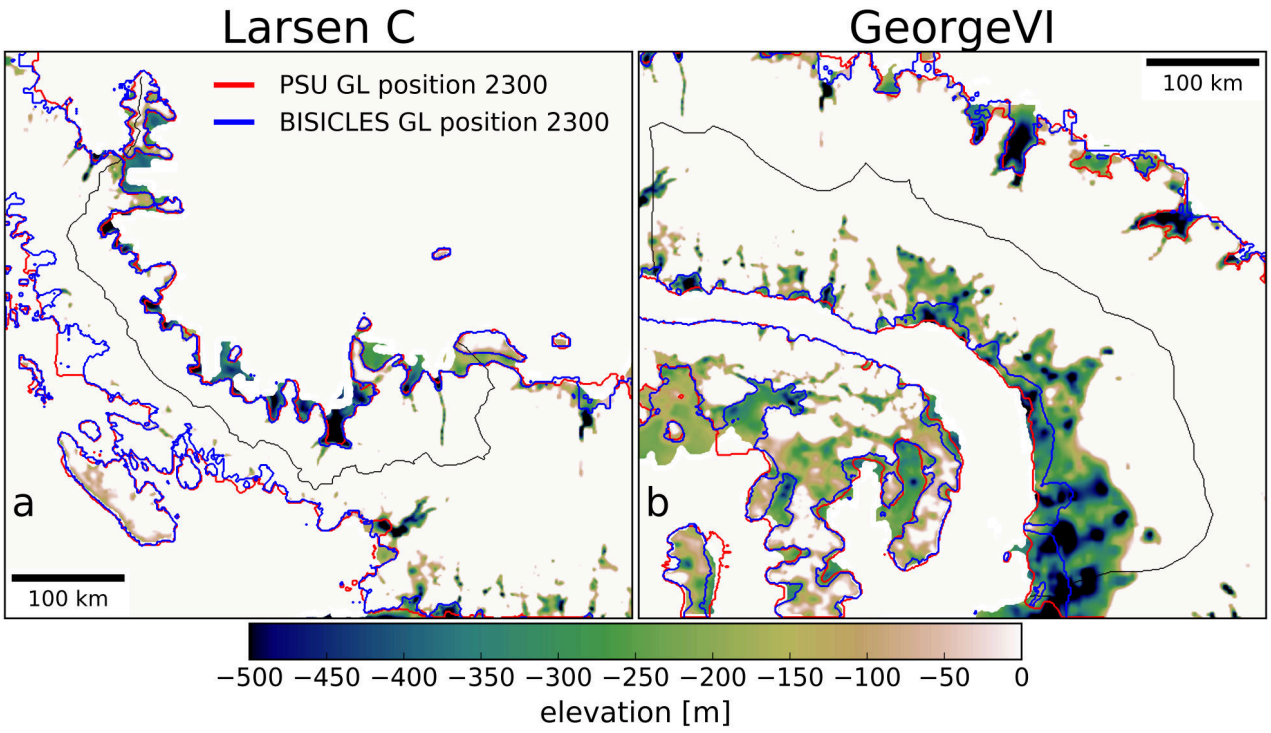

Figure A5. Comparison of modelled grounding-line positions from Experiment 2 (dynamic calving front) for RCP8.5 scenario for Larsen C (a) and George VI embayments (b). Black ~~line denotes~~ lines denote modelled drainage basins.

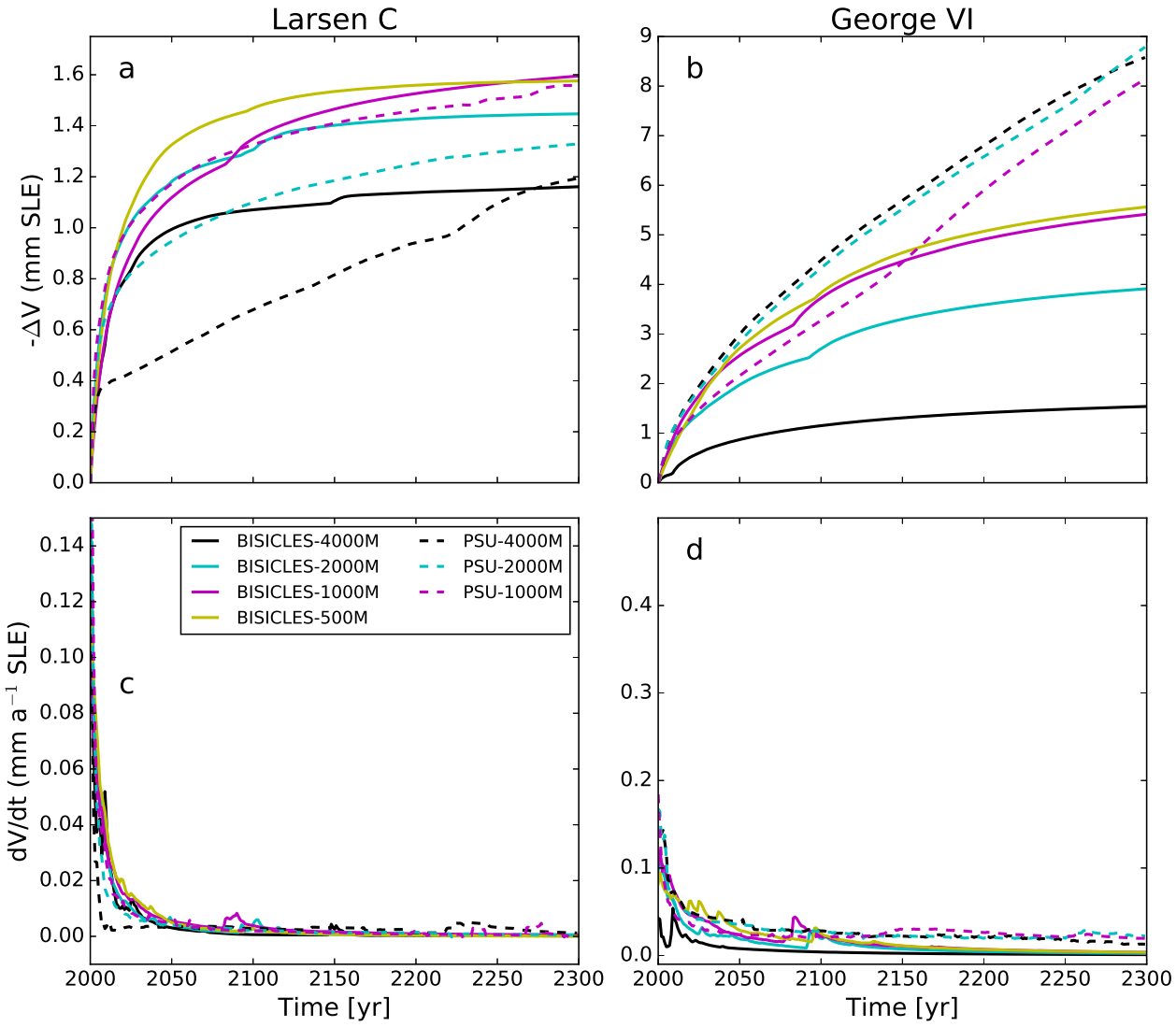

Figure A6. Upper ~~panel~~ panels (a,b) shows sea-level rise projections from Experiment 1 (immediate shelf collapse) at different horizontal resolutions for BISICLES (solid lines) and PSU3D (dashed lines). Lower ~~panel~~ panels (c,d) shows the derivative (rate of change) of the corresponding sea-level rise projections in the upper ~~panel~~ panels (a,b). Note different y-axis scales.

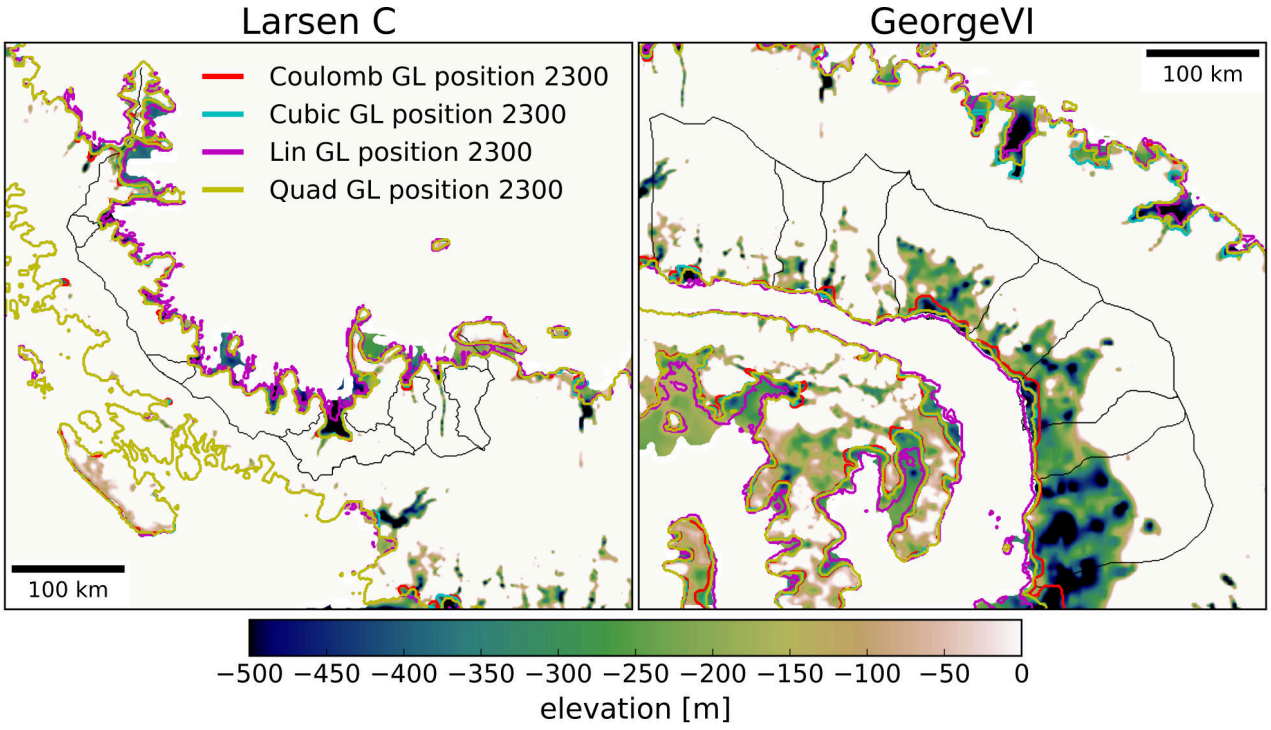

Figure A7. Comparison of modelled grounding-line positions using BISICLES with different basal sliding laws for Larsen C (a) and George VI embayments (b). Black ~~line denotes~~ lines denote modelled drainage basins.